

Boundary conditions for the order parameter and the proximity influenced internal phase differences in double superconducting junctions

Yu. S. Barash

*Institute of Solid State Physics of the Russian Academy of Sciences,
Chernogolovka, Moscow District, 2 Academician Ossipyan Street, 142432 Russia*

(Dated: August 30, 2022)

This paper gives an overview of the unconventional dependence of internal phase differences on the external phase difference in superconductor-normal metal-superconductor (SINIS) and superconductor-superconductor-superconductor (SISIS) tunnel double junctions. The results are obtained within the Ginzburg-Landau (GL) approach that includes boundary conditions for the superconductor order parameter in the presence of a Josephson coupling through interfaces. The boundary conditions are derived within the GL theory and substantiated microscopically. The absence of the one-to-one correspondence between external ϕ and internal $\chi_{1,2}$ phase differences in the junctions is shown to occur in two qualitatively different ways, both of which result in the range of $\chi_{1,2}$ reduced and prevent the 4π -periodic current-phase relation $j = j_c \sin \frac{\phi}{2}$. In SINIS junctions, the effect of the supercurrent-induced phase incursion φ between the end faces of the central electrode of mesoscopic length L can play a crucial role. In SISIS junctions, there occurs the regime of interchanging modes, which is modified as L decreases. The proximity and pair breaking effects in the double junctions with closely spaced interfaces are addressed.

1. INTRODUCTION

A phase dependent Josephson coupling of two superconductors linked to each other by quasiparticle tunneling through an interlayer, gives rise to the Josephson current through the system [1–3]. If two Josephson junctions, connected in series in a SISIS heterostructure, are at distance L that far exceeds the coherence length ξ , the coupling between them is negligible in the absence of magnetic effects. However, under the opposite condition $L \lesssim \xi$, the proximity and interface pair breaking can have a strong effect on the transport processes, including the Josephson current. Static and dynamic interactions of two closely spaced Josephson junctions can manifest in a variety of properties of mesoscopic superconducting heterostructures and play an important role in superconducting electronics [4–21].

When a normal metal is placed between the superconductors, the Josephson coupling emerges as a consequence of superconducting correlations generated by proximity effects in the normal metal region [22–26]. A number of hybrid systems with proximity-induced Josephson coupling through normal metal electrodes, have recently been the focus of scientific scrutiny [27–41].

The phase difference ϕ between external superconducting electrodes in symmetric superconducting double junctions incorporates the internal phase differences $\chi_{1,2}$ across the interfaces of constituent SIS or SIN junctions and the supercurrent-induced phase incursion φ between the end faces of the central electrode of length L : $\phi = \chi_1 + \chi_2 + \varphi$. Both the external and internal phase differences can be identified experimentally and controlled, although only one of them is usually an independent variable in the equilibrium state. Thus the internal phase difference can be controlled by the magnetic flux through a superconducting ring involving only one of two constituent contacts of a double junction.

However, the problem of internal phase differences has not yet received sufficient attention in the literature, whereas various other properties of SINIS and SISIS superconducting double junctions have been thoroughly developed and applied to a wide range of heterostructural parameters. One of the reasons for this is that the relation between the phase drops $\chi_{1,2}$ across the interfaces and the phase incursion φ over the central lead at a given ϕ is usually simplified, assuming negligible values of either φ , or $\chi_{1,2}$. For example, the more advanced early attempts to describe the SNS junctions within the Ginzburg-Landau (GL) approach [42, 43] considered the phase incursion and fully transparent interfaces, but used the specific boundary conditions and disregarded the phase drops. In particular, the boundary conditions (7) in Ref. [42], correct under the conditions studied, do not apply to the systems with the Josephson coupling. The boundary condition (5) in Ref. [43] is incorrect in general. On the other hand, in microscopic theories of the superconducting double junctions a negligible current-induced phase incursion is usually assumed, as distinct from the phase drops [10, 13, 26, 44]. Although the latter point is applied to SISIS junctions in a wide range of realistic parameters, the range gets narrower in SINIS junctions, where both $\chi_{1,2}$ and φ should, generally speaking, be taken into account for describing the transport at mesoscopic values of L [40].

Another aspect of the problem is that a fully self-consistent description should include the spatially dependent order parameter absolute value and its spatially dependent phase. This substantially complicates numerical simulations, as well as analytical calculations, since the phase changes incorporate sharp drops across thin interfaces and the phase incursion along the central electrode. An alternative approximate approach disregards the joint self-consistency

conditions and assumes the order parameter phase to be either spatially constant, or a linear function of coordinates inside each of the individual electrodes. The latter approach substantially simplifies the solution and, in a variety of cases, can be justified. However, an implicit assumption of such a standard approximation is the one-to-one correspondence between the external ϕ and internal $\chi_{1,2}$ phase differences, which recently has been demonstrated to be invalid under certain conditions in the double and multiple junctions [19, 20, 40]. The one-to-one correspondence gets broken in the SINIS and SISIS superconducting double junctions under two qualitatively different scenarios characteristic of the behavior of internal phase differences driven by the external phase difference and influenced by the proximity and pair breaking effects. It is one of the consequences of the broken correspondence that the 4π -periodic current-phase relation $j = j_c \sin \frac{\phi}{2}$, which is based on the simple equalities $\chi_{1,2} = \chi$, $j = j_c \sin \chi$, $\phi = 2\chi$, does not hold in the double tunnel junctions over the entire range of ϕ even when the phase incursion and proximity effects are negligibly small.

This paper gives an overview of the results relating to the internal phase differences in symmetric SINIS and SISIS double junctions, obtained within the GL approach involving the boundary conditions for the order parameter that take into account the Josephson coupling through interfaces [20, 40]. The problem of the corresponding boundary conditions will be discussed in detail below. Representing the self-consistency equation for the complex order parameter, the GL equations and boundary conditions offer the simplest way for describing the spatial distribution of both the order parameter's absolute value and its phase in superconducting heterostructures.

It is worth noting that if, in a problem, the specific GL temperature dependence of the quantities (i.e., their power-law dependence on $|T - T_c|$) is irrelevant, then as a rule, the corresponding results remain applicable on the semiquantitative level to a substantially wider temperature range compared to the GL temperature region near T_c [45]. This is expected to be the case in studying the internal phase differences and current-phase relations in both types of superconducting double junctions considered below within the GL theory.

The paper is organized in the following way: the Josephson coupling and the boundary conditions for the order parameter are both described within the GL theory and microscopically derived in Sec. 2; the phase relations in symmetric SINIS and SISIS superconducting double junctions are considered, based on the approach developed, in Secs. 3 and 4 respectively.

2. JOSEPHSON COUPLING AND BOUNDARY CONDITIONS IN THE GL THEORY

2.1. Symmetric Junctions between Identical Superconductors

The Josephson effect was successfully described within the GL theory first for the case of a superconducting point contact involving a fully transparent small constriction [46]. The focus of this paper is another standard type of superconducting junctions, where superconducting leads with identical constant cross sections are linked to each other by the quasiparticle transmission through planar interlayers with interfacial barriers. The Josephson part of the free energy functional near T_c , considered for the junction with a single thin interlayer, is the basis for getting the GL equations and boundary conditions at interfaces [47–51].

The phase dependent part of the Josephson interface free energy per unit area has a well-known bilinear form

$$\mathcal{F}_\chi^J = -g_J(\Psi_+\Psi_-^* + \Psi_-\Psi_+^*) = -2g_J|\Psi_-||\Psi_+|\cos\chi, \quad (1)$$

where the quantities $\Psi_\pm = |\Psi_\pm|e^{i\alpha_\pm}$ are the order parameter complex values on opposite interface sides, g_J is the Josephson coupling constant and $\chi = \alpha_- - \alpha_+$. Hereafter, the thickness of a homogeneous interlayer is assumed to be comparatively small for defining it to be zero within the GL theory. If the interlayer is placed at $X = X_{\text{int}}$, then $X_\pm = X_{\text{int}} \pm 0$. This does not exclude, for example, metallic interlayers with thicknesses on the order of the Cooper pair size.

When Eq. (1) is considered in the tunneling limit, the quantities $|\Psi_\pm|$ are taken in the zeroth-order approximation in powers of the Josephson coupling constant and are therefore independent of the phase difference χ . In this case one gets from (1) the standard textbook expression for the Josephson supercurrent density. In terms of the chosen notations

$$j = \frac{2|e|\hbar}{\hbar} \frac{d\mathcal{F}_\chi^J}{d\chi} = \frac{4|e|g_J}{\hbar} |\Psi_-||\Psi_+|\sin\chi. \quad (2)$$

For $g_J > 0$ this is a 0 junction, while one gets π junction for $g_J < 0$.

Although the phase-dependent interface free energy (1) incorporates important basic features of the Josephson effect, it generally disagrees with the microscopic theory since it does not take into account the accompanying proximity effects of the Josephson origin. The disadvantage originates from the incorrect condition, at which the Josephson free

energy part vanishes. Thus, assuming for identical superconducting leads equal order parameter values on opposite superconducting banks $|\Psi_{\pm}| = |\Psi|$ the Josephson junction energy is known to be proportional to $|\Psi|^2(1 - \cos \chi)$ and to vanish at $\chi = 0$ [52, 53]. The latter expression must be generalized in the GL theory to address the free energy variation due to independently changing order parameter values on opposite interface sides. The corresponding invariant term in the simplest case is

$$\mathcal{F}_s^J = g_J |\Psi_+ - \Psi_-|^2 = g_J \left[|\Psi_+|^2 + |\Psi_-|^2 - (\Psi_+ \Psi_-^* + \Psi_- \Psi_+^*) \right]. \quad (3)$$

The expression (3) implies the interlayer to be in the time-reversal invariant state and also symmetric with respect to the normal-axis inversion.

While the Josephson contribution (3) becomes proportional to $1 - \cos \chi$ and vanishes at zero phase difference $\chi = 0$ under the condition $|\Psi_+| = |\Psi_-|$, it does not vanish when $|\Psi_+| \neq |\Psi_-|$:

$$\mathcal{F}_{\chi=0}^J = g_J (|\Psi_+| - |\Psi_-|)^2. \quad (4)$$

If $g_J > 0$, the quantity $\mathcal{F}_{\chi=0}^J$ increases with a difference between the order parameter values $|\Psi_{\pm}|$. The associated proximity effect, that influences the near-interface order-parameter structure, can substantially differ from what would follow from (1).

The superconductivity can also be weakened (or enhanced) by its proximity to the boundary with an adjacent material, irrespective of the presence or absence of the supercurrent depairing and of the Josephson coupling over the boundaries. The surface depairing is known to occur, for example, near surfaces with normal metals and/or magnets [22, 47, 54–57]. Possible reasons for the surface superconductivity enhancement have been considered in Refs. [58–60] and references therein. The depairing effects in the near-surface region can also be associated with an anisotropic pairing structure in unconventional superconductors [61–71].

In the GL free energy with a single-component order parameter, terms of the form $g|\Psi_{\pm}|^2$ are responsible for the surface (interface) pair breaking at $g > 0$, or for enhancing the condensate density near the surface (interface) at $g < 0$. After adding the terms to the Josephson contribution (3), one gets the following quadratic form for the interface GL free energy per unit area

$$\mathcal{F}^{int} = (g + g_J)(|\Psi_+|^2 + |\Psi_-|^2) - g_J(\Psi_+ \Psi_-^* + \Psi_- \Psi_+^*). \quad (5)$$

As distinct from the bulk GL free energy, no terms involving the order parameter derivatives or its higher powers are usually required in the interface contributions (3) and (5), since neither of the corresponding coefficients vanishes there in view of the presumed absence of a zero-field quasi-two-dimensional phase transition in thin interfaces in question. Exclusions may concern small interface terms, not considered here, that result in qualitatively new kind of effect.

As seen in (5), the Josephson coupling constant g_J enters not only the phase-dependent expression (1), but also the pair breaking terms, where g_J is combined with g . This influences the near-surface spatial structure of the GL order parameter on the interface sides and contrasts to the standard analysis of the Josephson effect and boundary conditions within the GL theory, where the Josephson coupling was considered to be irrelevant to the surface pair breaking terms $\propto |\Psi_{\pm}|^2$ in the free energy. Therefore no such terms were assumed to appear in default of the surface pair breaking constant g , for example, in the case of conventional dielectric surfaces [47].

The boundary conditions are obtained in the GL theory from the vanishing free energy variation over the order parameter taken at a boundary or an interface side. As is well known, in addition to a surface or interface free energy, the bulk terms containing order parameter derivatives also contribute to the boundary conditions. Thus, in the simplest case discussed, the gradient bulk term $K|d\Psi(x)/dx|^2$ leads after the variation over $\Psi^*(x)$ not only to the second-order derivative $-Kd^2\Psi/dx^2$ in the GL equations for each of the electrodes, but also in the boundary terms $Kd\Psi/dx|_{x_2}$ and $-Kd\Psi/dx|_{x_1}$ that, respectively, enter the boundary conditions at the upper and the lower limits of the integration. Based on such a prescription and using (5), one gets the following boundary conditions for the order parameter on opposite sides of the interface

$$K \left(\frac{d\Psi}{dX} \right)_{\pm} = \pm(g + g_J)\Psi_{\pm} \mp g_J\Psi_{\mp}. \quad (6)$$

The contributions from the phase dependent Josephson coupling $\mp g_J\Psi_{\mp}$, from the surface pair breaking $\pm g\Psi_{\pm}$ and the interface proximity effects of the Josephson origin $\pm g_J\Psi_{\pm}$ have been taken into account on the right-hand side of the condition (6). The use of (1) instead of (5) would ignore both the surface pair breaking and the term $\pm g_J\Psi_{\pm}$, which can substantially distort the boundary condition.

When $g = 0$, (6) is reduced to

$$K \left(\frac{d\Psi}{dX} \right)_{\pm} = g_J (\Psi_+ - \Psi_-). \quad (7)$$

Here the derivative of the order parameter, taken on one side of the interface with the corresponding coefficient, is linked by the Josephson coupling strength with the difference between the order parameter values on the two interface sides.

The boundary conditions (6) have been used for describing single and double Josephson junctions within the GL theory [20, 40, 72–77].

2.2. Junctions with the Broken Symmetries

One might think that the Josephson coupling-induced free energy (3) applies also to a junction with electrodes made of different superconducting materials. This is generally not the case as is evidenced by the fact that changing the material dependent normalization of the order parameter in (3) results not only in a re-defining of the coefficient g_J , but also in an additional independent parameter associated with the difference between normalization factors on the opposite sides of the interface. A well-known change of the normalization factor is associated with switching from the gap function to the standard GL order parameter [78–80]. Although a joint consideration of different superconducting materials within the GL theory is known to be seriously restricted by the requirement that their critical temperatures $T_{c\pm}$ must be close to each other, various other independent material parameters can differ substantially. This concerns both SIS' junctions at $T < T_{c\pm}$ and SIN junctions at $T_{c-} < T < T_{c+}$ [80].

Therefore, one should write a generalized version of (3):

$$\mathcal{F}^J = |\beta_+ \Psi_+ - \beta_- \Psi_-|^2. \quad (8)$$

Here β_{\pm} are real coefficients that can have identical or opposite signs.

Introducing $g_J = \beta_+ \beta_-$ and $g_{J\pm} = |\beta_{\pm}|^2$, one obtains from (8)

$$\mathcal{F}^J = g_J |\Psi_+ - \Psi_-|^2 + (g_{J+} - g_J) |\Psi_+|^2 + (g_{J-} - g_J) |\Psi_-|^2. \quad (9)$$

Unlike (3), a change of the order parameter normalization in (8) or (9) does not result in new terms, but only in the re-defining of the coefficients β_{\pm} , g_J and $g_{J\pm}$.

The expression (9) also applies to the case of an interlayer with the broken normal-axis inversion. After adding to (9) the surface pair-breaking terms $g_{\pm}^{\text{surf}} |\Psi_{\pm}|^2$ and introducing notations $g_{\pm} = g_{\pm}^{\text{surf}} + (g_{J\pm} - g_J)$, one gets for the interface free energy

$$\mathcal{F}^{\text{int}} = (g_+ + g_J) |\Psi_+|^2 + (g_- + g_J) |\Psi_-|^2 - g_J (\Psi_+ \Psi_-^* + \Psi_- \Psi_+^*). \quad (10)$$

The boundary conditions that follow from (10) are

$$K_+ \left(\frac{d\Psi}{dX} \right)_+ = (g_+ + g_J) \Psi_+ - g_J \Psi_-, \quad (11)$$

$$K_- \left(\frac{d\Psi}{dX} \right)_- = g_J \Psi_+ - (g_- + g_J) \Psi_-. \quad (12)$$

The free energy (10) and the boundary conditions (11), (12) are similar to (5) and (6), respectively. The difference is associated with distinct coefficients g_{\pm} of the pair breaking terms on opposite interface sides compared with a common coefficient g in (5) and (6) in symmetric junctions. In the absence of surface contributions $g_{\pm}^{\text{surf}} = 0$, the quantities g_{\pm} do not vanish here due to the finite differences $g_{J\pm} - g_J$ of the Josephson origin.

It is worth noting that in a more involved case of chiral interlayers with the broken time reversal symmetry, the coefficients in (8) can take complex values $\beta_{\pm} = |\beta_{\pm}| e^{i\gamma_{\pm}}$ with different phases γ_{\pm} . The corresponding interface free energy is

$$\mathcal{F}^{\text{int}} = (g_{J+} + g_+) |\Psi_+|^2 + (g_{J-} + g_-) |\Psi_-|^2 - 2g_J |\Psi_- \Psi_+| \cos(\chi - \chi_0), \quad (13)$$

where $g_{J\pm} = |\beta_{\pm}|^2$, $g_J = |\beta_+ \beta_-|$, $\chi_0 = \gamma_+ - \gamma_-$.

The associated boundary conditions are

$$K_+ \left(\frac{d\Psi}{dX} \right)_+ = (g_+ + g_{J+})\Psi_+ - g_J e^{-i\chi_0} \Psi_-, \quad (14)$$

$$K_- \left(\frac{d\Psi}{dX} \right)_- = g_J e^{i\chi_0} \Psi_+ - (g_- + g_{J-})\Psi_-. \quad (15)$$

The anomalous Josephson current, which is proportional to $\sin(\chi - \chi_0)$ in the tunneling limit, follows from (13) in agreement with what is known for such a case [81–85]. A joint effect of the interfacial spin-orbit coupling and exchange field can also induce the spontaneous boundary currents [86], described by introducing an additional specific first-order gradient term in the GL interface free energy [87–90]. Since both the latter effect and the anomalous Josephson effect itself are beyond the scope of this paper, complex values of β_{\pm} will not be considered below.

2.3. The Josephson Coupling in the GL Theory: a Microscopic Viewpoint

Quasiclassical theory of dirty superconductors probably offers the simplest way for a microscopic derivation of the boundary conditions for the GL order parameter. Thus the Kupriyanov-Lukichev boundary conditions, which are known to be applied within the Usadel approach to the Green functions at tunnel interfaces [44], can be linearized in the anomalous Green function F as it becomes small near T_c . Focusing on symmetric tunnel junctions with identical superconducting electrodes one obtains the following linearized relationship

$$\frac{\sigma}{G_N} \left(\frac{dF}{dX} \right)_{\pm} = F_+ - F_-. \quad (16)$$

Here G_N is the interface conductance per unit area and σ is the normal-state conductivity of the superconducting leads.

Similarly to Subsec. 2.2.1, it is presumed in (16) that the first-order terms dominate the boundary conditions near T_c . Since the anomalous Green function F and the gap function Δ are both small near T_c , and their spatial derivatives introduce additional small factors, the relation $\Delta = \omega F$, where ω is the Matsubara frequency, follows, in the first approximation, from the Usadel equations. Therefore, the boundary condition for the gap function does not change as compared to (16):

$$\frac{\sigma}{G_N} \left(\frac{d\Delta}{dX} \right)_{\pm} = \Delta_+ - \Delta_-. \quad (17)$$

The same result can also be obtained from (16) based on the self-consistency condition

$$\Delta(x) = \pi\lambda T \sum_{|\omega| < \omega_D} F(x, \omega). \quad (18)$$

Here the BCS coupling constant λ and the Debye frequency ω_D of the superconducting electrodes enter the equality.

Eq. (17) has a form of the GL boundary conditions (7) applied to symmetric junctions with no surface pair breaking, i.e., at $g = 0$. The gap function near T_c is known to play the role of the order parameter and to differ from the standard GL order parameter Ψ only by the normalization factor and the associated modified microscopic definitions of GL coefficients [78–80]. For junctions with identical superconducting electrodes those normalization factors cancel each other out, and the boundary condition for the standard GL order parameter Ψ coincides with (17)

$$\frac{\sigma}{G_N} \left(\frac{d\Psi}{dX} \right)_{\pm} = \Psi_+ - \Psi_-. \quad (19)$$

One can also introduce in (7) and (19) the dimensionless coordinate $x = X/\xi$, where ξ is the superconductor coherence length, and rewrite the equalities as

$$\left(\frac{d\Psi}{dx} \right)_{\pm} = \frac{\xi g_J}{K} (\Psi_+ - \Psi_-) = g_{\ell} (\Psi_+ - \Psi_-), \quad (20)$$

$$\left(\frac{d\Psi}{dx} \right)_{\pm} = \frac{\xi G_N}{\sigma} (\Psi_+ - \Psi_-). \quad (21)$$

Comparing the microscopic and the GL boundary conditions (19) and (7), as well as the associated equalities (20) and (21), leads to the following expressions

$$g_J = \frac{KG_N}{\sigma}, \quad g_\ell = \frac{\xi G_N}{\sigma}. \quad (22)$$

Therefore, the condition $\xi G_N/\sigma \ll 1$, which is known to allow the junction description in the tunneling limit, is rewritten in terms of g_ℓ as $g_\ell \ll 1$.

Microscopic expressions for g_J , g_ℓ can also be obtained by comparing microscopic results for the Josephson current near T_c with the corresponding formulas of the GL theory. In the absence of surface pair breaking, the GL expression for the critical current in the tunneling limit $j_c = \frac{4|e||a|}{\hbar b} g_J$, that applies to symmetric SIS tunnel junctions, follows from (2) after substituting there the conventional bulk GL expression $|\Psi_\pm|^2 = |a|/b$ for the equilibrium order parameter via the standard GL coefficients (see, e.g., (56)). On the other hand, the microscopic Ambegaokar-Baratoff formula near T_c for the same system can be represented as $j_c = \pi|\Delta|^2 G_N/4|e|T_c$, where the BCS gap function in the bulk near T_c is $|\Delta|^2 = 8\pi^2 T_c(T_c - T)/(7\zeta(3))$ [91]. Thus, equating the two expressions and using the relation $|a| = \alpha|T_c - T|/T_c$ one gets

$$g_J = \frac{\pi^3 \hbar b T_c G_N}{14\zeta(3) e^2 \alpha}. \quad (23)$$

Eq. (23) can be specified further with the Gor'kov's microscopic formulas for b/α in the clean and dirty limits [78, 79]. Substituting the simplest expression $G_N = e^2 k_F^2 \overline{\mathcal{D}}/4\pi^2 \hbar$, that connects the junction conductance with the averaged transmission coefficient $\overline{\mathcal{D}}$, one gets for pure junctions $g_\ell = 3\pi^2 \overline{\mathcal{D}} \xi(T)/(14\zeta(3)\xi_0) = 1.76 \overline{\mathcal{D}} \xi(T)/\xi_0$. Here $\xi_0 = \hbar v_F/\pi T_c$ is the zero-temperature coherence length and v_F , k_F are the Fermi velocity and wave vector. Based on (23) and the microscopic expression for b/α for dirty junctions and using the relations $K = \hbar^2/4m$, $\sigma = n_e e^2 l_{\text{imp}}/p_f$, where l_{imp} is the mean free path, one obtains the same results (22) derived above with the Kupriyanov-Lukichev boundary conditions. Further substitution of the expression for G_N in (22) results in $g_\ell = 0.75 \overline{\mathcal{D}} \xi(T)/\ell$.

The estimates made above also agree with the microscopic formulas obtained long ago for boundary conditions for the order parameter near T_c in the tunneling limit [92–94]. The estimate $g_\ell \sim \overline{\mathcal{D}} \xi(T)(l_{\text{imp}}^{-1} + \xi_0^{-1})$, that sometimes is identified as the effective transparency [95, 96], applies not only to junctions in the tunneling limit $g_\ell \ll 1$ but also to those with moderate transparency not too close to unity. As the ratio $\xi(T)/l$ in dirty superconductors can be ~ 100 even at low temperatures, the quantity $g_\ell \sim \overline{\mathcal{D}} \xi(T)/l$ can vary, for small and moderate transparencies, from vanishingly small values in the tunneling limit to those well exceeding 100 near T_c , when a pronounced anharmonic behavior of the Josephson current is known to take place [72, 74, 76, 97]. In highly transparent junctions, for which $1 - \mathcal{D} \ll 1$, the parameter $g_\ell \propto (1 - \mathcal{D})^{-1}$ can be very large, as follows from microscopic results for the Josephson current in planar junctions with thin interlayers [55, 92–94, 97] (see also [26, 98]).

3. INTERNAL PHASE DIFFERENCES IN SINIS DOUBLE JUNCTIONS

3.1. Basic Equations

This section presents a theory of the reduced range of changes and unconventional behaviors of internal phase differences $\chi_{1,2}$ across the two interfaces in symmetric SINIS double tunnel junctions, that occur under the effect of controlled variations of either the external phase difference ϕ between superconducting terminals, or the quantities $\chi_{1,2}$ themselves.

The interfaces are set upon the end faces of the central normal metal lead of length L (see Fig. 1). A one-dimensional spatial dependence of the order parameter is considered, as it is assumed that the transverse dimensions of the electrodes are significantly smaller than the superconductor coherence length ξ and the decay length ξ_n in the normal metal electrode. The system's free energy consists of the bulk and interface terms $\mathcal{F} = \sum \mathcal{F}_p + \mathcal{F}_n + \mathcal{F}_{\frac{n}{2}}^{\text{int}} + \mathcal{F}_{-\frac{n}{2}}^{\text{int}}$. Here $p = 1, 2$ correspond to the external superconducting electrodes, while subscript n - to the central normal metal lead.

For the central electrode, one can write the following bulk GL free energy per unit area of the cross section

$$\mathcal{F}_n = \int_{-L/2}^{L/2} dX \left[K_n \left| \frac{d}{dX} \Psi(X) \right|^2 + a_n |\Psi(X)|^2 + \frac{b_n}{2} |\Psi(X)|^4 \right], \quad (24)$$

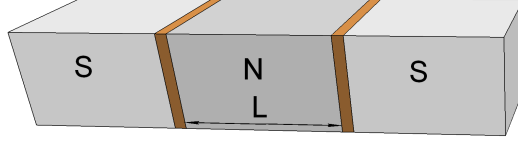


Figure 1: Schematic diagram of the SINIS junction. Adopted from Ref. [40].

where $K_n, a_n, b_n > 0$ and the interfaces are situated at $X = \pm L/2$. The expressions for $\mathcal{F}_{1,2}$ can be obtained from (24) by substituting $K, -|a|, b$ for K_n, a_n, b_n , respectively, and replacing the integration period $(-L/2, L/2)$ by $(-\infty, -L/2)$ or $(L/2, \infty)$ for $p = 1$ or 2 .

The interface terms in the free energy per unit area at $X = \pm L/2$ are similar to (10):

$$\mathcal{F}_{\pm \frac{L}{2}}^{\text{int}} = g_J \left| \Psi_{\pm(\frac{L}{2}+0)} - \Psi_{\pm(\frac{L}{2}-0)} \right|^2 + g \left| \Psi_{\pm(\frac{L}{2}+0)} \right|^2 + g_n \left| \Psi_{\pm(\frac{L}{2}-0)} \right|^2. \quad (25)$$

The GL equation for the normalized absolute order-parameter value can be written as

$$\begin{cases} \frac{d^2 f}{dx^2} - \frac{i^2}{f^3} - f - f^3 = 0, & |x| < l/2, \\ \frac{d^2 f}{dx^2} - \frac{K_n^2}{K^2} \cdot \frac{i^2}{f^3} + \frac{|a|K_n}{a_n K} f - \frac{bK_n}{b_n K} f^3 = 0, & |x| > l/2. \end{cases} \quad (26)$$

Here the dimensionless quantities f and x are defined as $\Psi = (a_n/b_n)^{1/2} f e^{i\alpha}$, $x = X/\xi_n(T)$. Also $l = L/\xi_n$, $\xi_n(T) = (K_n/a_n)^{1/2}$ and the dimensionless current density is $i = \frac{2}{3\sqrt{3}}(j/j_{\text{dp}})$, where $j_{\text{dp}} = (8|e|a_n^{3/2}K_n^{1/2})/(3\sqrt{3}\hbar b_n)$. One also assumes $a_n \sim |a|$ that makes possible a joint description of the normal metal and superconducting leads within the GL approach [80].

The boundary conditions for the complex order parameter, obtained from (24), (25) on the interfaces at $x = \pm l/2$, are reduced to following equalities for real quantities

$$\begin{cases} \left(\frac{df}{dx} \right)_{\pm(l/2-0)} = \mp (g_{n,\delta} + g_\ell) f_- \pm g_\ell f_+ \cos \chi, \\ \frac{K}{K_n} \left(\frac{df}{dx} \right)_{\pm(l/2+0)} = \pm (g_\delta + g_\ell) f_+ \mp g_\ell f_- \cos \chi, \end{cases} \quad (27)$$

$$i = -f^2 \frac{d\alpha}{dx} = g_\ell f_- f_+ \sin \chi. \quad (28)$$

Here the subscripts $+$ and $-$ in f_\pm correspond to the superconducting and normal metal banks respectively. The dimensionless coupling constants are

$$g_\ell = g_J \xi_n(T)/K_n, \quad g_{n,\delta} = g_n \xi_n(T)/K_n, \quad g_\delta = g \xi_n/K_n \quad (29)$$

and the symmetric solutions $f(x) = f(-x)$ are considered.

3.2. Phase Relations in SINIS Junctions

If a superconducting order parameter f_+ is present on one of the sides of a thin interface and the condition $g_\ell \cos \chi > 0$ is satisfied, then the bilinear part of the Josephson free energy $\propto -2g_\ell f_- f_+ \cos \chi$ (see (25) and (1)) decreases with an appearance of a small nonzero order parameter f_- on the other side. This results in the proximity effect of the

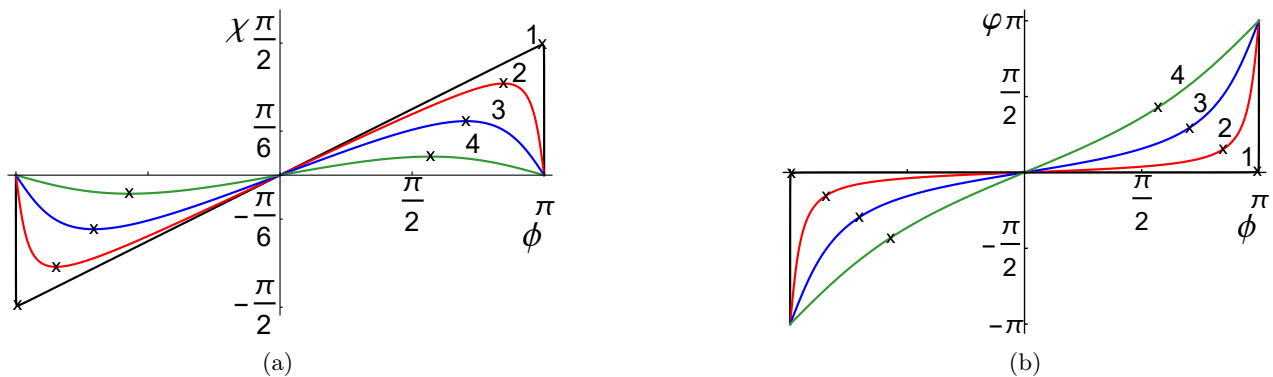


Figure 2: The internal phase difference χ (a) and the phase incursion φ (b) as functions of the external phase difference ϕ taken at various central lead's lengths l : (1) $l = 0.02$ (2) $l = 0.5$ (3) $l = 1.1$ (4) $l = 2.2$. Adopted from Ref. [40].

Josephson origin related to the term with $\cos \chi$ in the boundary conditions (27). Therefore, for superconductivity to emerge on the opposite interface side in the normal metal lead, in the presence of 0-junctions considered below ($g_\ell > 0$), the internal phase difference χ must take its values within the proximity-reduced range $|\chi| \leq \chi_{\max}(l) < \frac{\pi}{2}$ defined modulo 2π . Outside the range, the Josephson coupling would prevent superconductivity to appear in the normal metal lead.

The internal phase difference $\chi = \chi_{1,2}$ and the phase incursion φ taken at various l , are shown in Figs. 2(a) and 2(b), respectively, as functions of the external phase difference ϕ . The numerical results shown have been obtained by evaluating the GL equations' solutions with $g_\ell = g_\delta = 0.01$, $g_{n,\delta} = 0$, $K = K_n$, $|a| = a_n$ and $b = b_n$. The analytical solutions, presented in Subsec. 3.3.5 for tunnel SINIS junctions, approximate almost perfectly the quantities $\chi(\phi)$ and $\varphi(\phi)$ for the parameter set considered, with deviations from the numerical results that are indiscernible in Figs. 2(a) and 2(b).

A simple relationship $\chi(\phi) = \frac{\phi}{2}$, which follows from the equality $\phi = 2\chi + \varphi$ in the case of negligibly small phase incursion, results in the variation range $|\chi| \leq \frac{\pi}{2}$ for $|\phi| \leq \pi$. As seen in the curves 1 in Figs. 2(a) and 2(b), such behavior occurs at sufficiently small lengths $l \ll 1$, except for small vicinities of $\phi = \pm\pi$. The curves 2-4 show that the internal phase difference χ substantially contributes to the phase relations in a wide range of ϕ and at mesoscopic lengths $l \lesssim 1$, while φ is of importance at $l \gtrsim 1$.

Due to a spatially constant supercurrent occurring in the quasi-one-dimensional problem considered, a local decrease of the condensate density leads to the increase of the superfluid velocity, i.e., of the gradient of the order parameter phase. In this regard, a spatial decay of the proximity-induced Cooper pair density that takes place inside the central electrode as a distance from the nearest interface increases, plays an important role. This is the origin of a noticeable phase incursion taking place in a wide range of the phase difference ϕ in SINIS double junctions with a central lead of a mesoscopic length l . Smaller local values of f near the lead's center at larger l increases the phase incursion φ at a given ϕ , while the range of variation of χ diminishes $|\chi| \leq \chi_{\max}(l)$. In accordance with the result (45) of Subsec. 3.3.5, $\chi_{\max}(l) \approx \arccos(\tanh l)$. When $l \gg 1$, the order parameter is especially small in the depth of the central electrode and the phase incursion φ dominates χ in the equality $\phi = 2\chi + \varphi$, while $|\chi|$ is greatly reduced.

As seen in Fig. 2(a), the internal phase difference χ is a nonmonotonic function of the external phase difference ϕ . With ϕ changing over the period, χ passes through its proximity-reduced region twice, there and back. Two different values of ϕ , that correspond to one and the same χ , and to different phase incursions, belong to the two solutions of the GL equation for the absolute value of the order parameter, taken at a given χ . In all the figures, the dots marked with crosses indicate the points of contact of the two solutions, i.e., the quantities taken at $\chi = \pm\chi_{\max}(l)$.

3.3. The Proximity-Induced Phase Dependent Order Parameter

The nonlinear term $i^2 f^{-3} \propto v_s^2(x)f(x)$, that takes into account an influence of the conserved supercurrent on the proximity effect, i.e., on the induced order parameter in the normal metal electrode, cannot, as a rule, be neglected in (26) in comparison with the linear term. When ϕ is close to π , it dominates the latter in the depth of the central lead (see (50) and its discussion in Subsec. 3.3.5). Thus, the GL equation (26) is a nonlinear one even if the conventional cubic term is negligible in the problem in question. Although in the latter case the equation for the complex order parameter amplitude is still linear, the nonlinearity appears in describing the order parameter's absolute value and

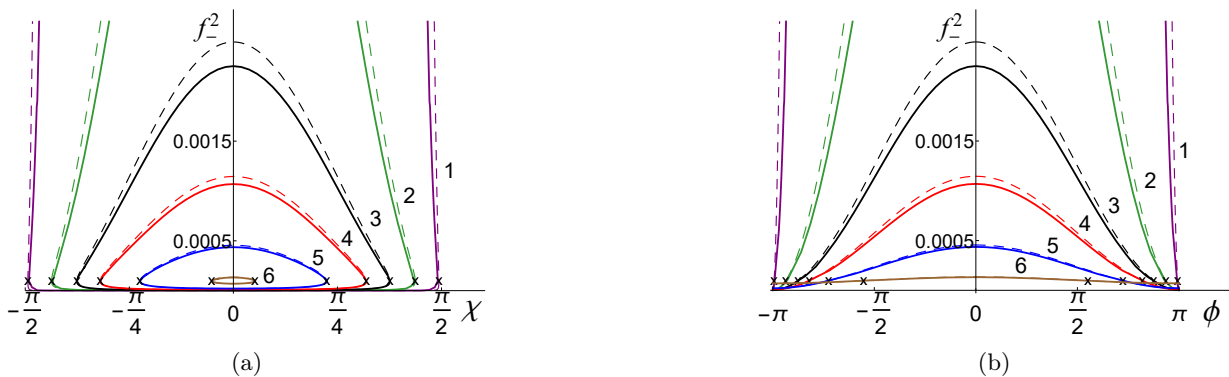


Figure 3: The quantity f_-^2 as (a) a double-valued function of χ and (b) a single-valued function of ϕ taken at various l : (1) $l = 0.02$ (2) $l = 0.2$ (3) $l = 0.4$ (4) $l = 0.6$ (5) $l = 1$ (6) $l = 2.5$. Adopted from Ref. [40].

phase. As a result of the nonlinearity, two basic solutions for f at a given χ will be shown to take place in the problem even for very small order parameter values. However, in the absence of a sizable spatially dependent gauge invariant gradient of the order parameter phase that is linked with the order parameter absolute value by the current conservation condition, the linearization represents the simplest and most effective way of solving the problems of H_{c2} and H_{c3} [52, 99, 100] as well as of the proximity effects near superconductor-normal metal boundaries [80, 101].

Figures 3(a) and 3(b) show the normalized order parameter absolute value squared f_-^2 , taken on the end face of the central electrode at various l , as a function of χ and ϕ , respectively. Solid curves give the numerical results obtained within the same framework as in Fig. 2. Dashed curves depict the analytical results of Subsec. 3.3.5, that assume the conditions $f_- \sim g_\ell f_+ \ll 1$, $g_{n,\delta} \lesssim g_\ell$ and lead to (38), (42) - (44), (53). They approximate the numerical results reasonably well. Unlike the phase relations in Fig. 2, the solid and dashed curves in Fig. 3 can be, for the most part, clearly distinguished. The double-valued behavior shown in Fig. 3(a) is described by the two solutions for f_-^2 adjoining at $\chi = \pm\chi_{\max}(l)$. The first solution has the maximum value and the second one the minimum at $\chi = 0$ at a fixed l . A similar behavior takes place at $l \rightarrow 0$ at a fixed χ , where the minimum is zero.

If χ were the control parameter in an experiment, the first solution would represent the stable states and the second one the metastable states. However, the external phase difference ϕ is usually fixed experimentally. After switching over from χ to ϕ , the two solutions occupy different regions within the period, adjoining at the points $\phi = \pm\phi_*(l)$. They jointly form the continuous single-valued order parameter behavior $f_-(\phi, l)$ shown in Fig. 3(b). The first solution incorporates $|\phi| \in (0, \phi_*(l))$ while the second one is in $|\phi| \in (\phi_*(l), \pi)$. Here $\phi_*(l) \approx \frac{\pi}{2} + \arcsin(\frac{1}{\cosh l})$, in accordance with (54), and the adjoining regions do not overlap due to a pronounced phase incursion taking place at small f . The curves' crossing at small f_- , shown in Fig. 3(b), is a consequence of different behavior of the two solutions with increasing l . Phase-slip processes in the central lead can take place at $\phi = \pm\pi$ and at arbitrary l , as in this case f vanishes at $x = 0$ [38, 43] (see also (50)). This results in a noticeable phase incursion in immediate vicinities of $\phi = \pm\pi$ even at small values of l .

The quantity f_+ changes weakly with χ and l : $f_+^2 \in (0.972, 0.978)$ for the whole parameter set used in the figures. For tunnel interfaces the estimate $f_- \sim g_\ell f_+ \ll 1$ holds at $g_{n,\delta} \lesssim g_\ell$, with the exception of the first solution at sufficiently small l . In the limit of small l , the first solution satisfies the relation

$$f_- = \frac{g_\ell \cos \chi}{g_\ell + g_{n,\delta}} f_+, \quad (30)$$

which assumes $\cos \chi \geq 0$ and approximately describes the dependence of f_- on χ and also applies to SISIS junctions [20].

If $g_{n,\delta} \lesssim g_\ell$ and $\cos \chi \sim 1$, it follows from (30) $f_- \sim f_+$. In the opposite case $g_{n,\delta} \gg g_\ell$ one gets $f_- \ll f_+$. Since g_ℓ for tunnel interfaces is proportional to the transmission coefficient $g_\ell \propto \mathcal{D}$ (see Subsec. 2.2.3), one obtains from (30) $f_- \propto \mathcal{D}$, if $g_\ell \ll g_{n,\delta}$, and the \mathcal{D} -independent quantity f_- for $g_\ell \gg g_{n,\delta}$. The second solution vanishes in the limit $l \rightarrow 0$, and satisfies the relation $f_- = g_\ell f_+ \tanh \frac{l}{2}$ at arbitrary l and $\chi = 0$. The two solutions for large l coincide and the relation at $\chi = 0$ is $f_- = g_\ell f_+$ (see Supplemental Material in Ref. [40]).

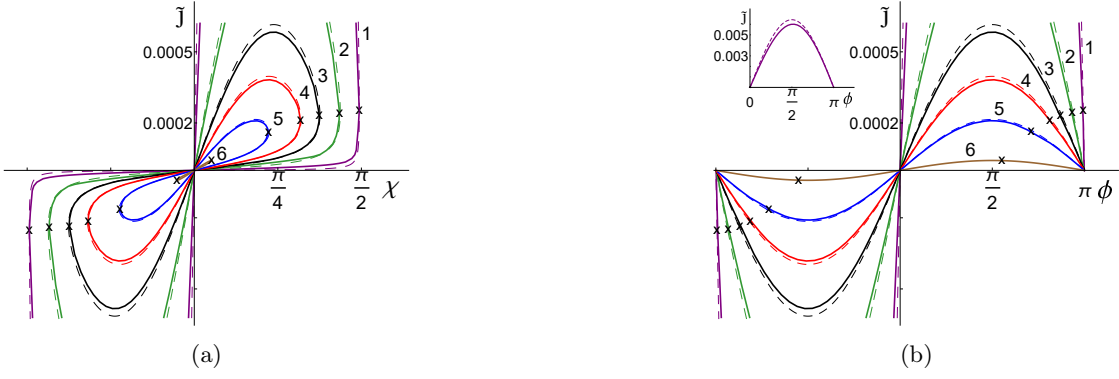


Figure 4: Normalized supercurrent as (a) a double-valued function of χ and (b) a single-valued function of ϕ taken at various l : (1) $l = 0.02$ (2) $l = 0.2$ (3) $l = 0.4$ (4) $l = 0.6$ (5) $l = 1$ (6) $l = 2.5$. Inset: The supercurrent at $l = 0.02$ (solid line) and its analytical description at small l (dashed line). Adopted from Ref. [40].

3.4. Dependence of the Supercurrent on Internal Phase Differences in SINIS

The normalized supercurrent $\tilde{j} = j/j_{\text{dP}}$ as a function of χ and ϕ is depicted at various l in Figs. 4(a) and 4(b), respectively. With varying χ , the curves have the form of a double loop looking like a sloping figure eight composed of the two solutions. By contrast, after switching from χ to ϕ the transformed curves correspond to the conventional current-phase relation. The dashed curves are based on the approximate analytical results of Subsec. 3.3.5. They deviate by several percent from the numerical solutions (solid curves) having the sinusoidal shape in Fig. 4(b).

A role of the phase incursion in producing the obtained phase-dependent behavior can be explained as follows. The factor f_- in the supercurrent $i = g_\ell f_- f_+ \sin \chi$ is most sensitive to the proximity effect. If φ were negligibly small, the value of the external phase difference $\phi = \pi$ would correspond to $\chi = \frac{\pi}{2}$. Since the bilinear part of the Josephson free energy $\propto -2g_\ell f_- f_+ \cos \chi$ and the corresponding proximity effect vanish at $\chi \rightarrow \frac{\pi}{2}$, one obtains $f_- \rightarrow 0$ that entails the zeroth supercurrent at $\phi = \pi$. At the same time, small values of f_- in the vicinity of $\phi = \pi$ result in a noticeable phase incursion. In view of the relation $\chi = (\phi - \varphi)/2$, the phase incursion diminishes the variation range $|\chi| \leq \chi_{\text{max}}(l) < \frac{\pi}{2}$ that prohibits χ to reach $\frac{\pi}{2}$ at any nonzero l . Instead, two solutions of the GL equation provide a return passage for χ , from 0 to $\chi_{\text{max}}(l)$ and back, when ϕ changes over $(0, \pi)$. This results in the correspondence of $\chi = 0$ to both $\phi = 0$ and $\phi = \pi$.

Since the analytical results of Subsec. 3.3.5 can only be justified for sufficiently small g_ℓ , the small Josephson coupling constant $g_\ell = 0.01$ has been chosen to demonstrate a quantitative agreement with the numerical data. The chosen g_ℓ leads to small values of the order parameter f_- and the supercurrent, which pertain to the second solution and are depicted in Figs. 3 and 4 below the points marked with crosses. The effects in question increase with g_ℓ and remain qualitatively the same for $g_\ell \lesssim 1$. For example, for $g_\ell = 0.1$ instead of $g_\ell = 0.01$, the typical values of f_-^2 and \tilde{j} increase in about 50 – 100 times.

The first solution is substantially modified at small length of the central lead $l \lesssim 2g_\ell(b_n|a|/ba_n)^{1/2} \ll 1$. The corresponding analytical description should be based on the relation (30) rather than on $f_- \sim g_\ell f_+ \ll 1$ (see Supplemental Material in Ref. [40]). The solid curve 1 as a whole ($l = 0.02$) is shown in the inset in Fig. 4(b). It is well approximated by the analytical results. Under the condition $g_{n,\delta} \ll g_\ell$, one obtains $j \propto \mathcal{D}$ from (30). However, the supercurrent dependence on the transparency is gradually transformed into \mathcal{D}^2 with increasing ϕ up to about ϕ_* at a fixed small l , when the relation $f_- \sim g_\ell f_+ \ll 1$ comes into play along with the increase of the phase incursion. The second solution always results in $j \propto \mathcal{D}^2$. The crossover obtained is a fingerprint of the phase-dependent proximity effect of the Josephson origin that results in an unconventional behavior of internal phase differences in SINIS junctions. A similar behavior of a supercurrent also occurs with the increasing distance l at a fixed ϕ [10, 13, 26, 44].

3.5. Analytical Results for Tunnel SINIS Junctions

This section focuses on the analytical results used above for plotting the dashed curves in Figs. 2 - 4. For a more complete analytical consideration of the problem see Supplemental Material in Ref. [40].

The GL equation and boundary conditions, applied to the complex order parameter with one dimensional spatial dependence, lead not only to the equations (26), (27), but also to additional equalities, that ensure the conservation of the current through both the superconducting leads and the interfaces. The equalities can be written in the form

of (28) and as

$$i^2 = \frac{Kb}{K_n b_n} \left(\frac{|a|b_n}{a_n b} - f_\infty^2 \right) f_\infty^4. \quad (31)$$

The first expression in the right-hand side of (28) is the normalized standard GL expression for the supercurrent, which is valid everywhere inside the leads. The second expression in (28) is the supercurrent value at the boundary, as it follows from the boundary condition for the complex order parameter. The expression (31) for i^2 is obtained from (26) in the limit $x \rightarrow \infty$, in view of the relation $df/dx \rightarrow 0$.

The asymptotic order parameter value generally depends on the supercurrent. Equating (28) and (31) results in

$$\frac{Kb}{K_n b_n} \left(\frac{|a|b_n}{a_n b} - f_\infty^2 \right) f_\infty^4 = g_\ell^2 f_-^2 f_+^2 \sin^2 \chi. \quad (32)$$

In the currentless state with $\chi = 0, \pi$ one gets from (32) for the normalization chosen

$$f_\infty^2 = \frac{|a|b_n}{a_n b}. \quad (33)$$

The first integrals \mathcal{E}_n and \mathcal{E} of the GL equations (26), which are usually useful for analyzing the solutions, are

$$\mathcal{E}_n = \left(\frac{df(x)}{dx} \right)^2 + \frac{i^2}{f^2(x)} - f^2(x) - \frac{1}{2} f^4(x), \quad |x| < l/2, \quad (34)$$

$$\mathcal{E} = \left(\frac{df(x)}{dx} \right)^2 + \frac{K_n^2}{K^2} \frac{i^2}{f^2(x)} + \frac{|a|K_n}{a_n K} f^2(x) - \frac{bK_n}{2b_n K} f^4(x), \quad |x| > l/2, \quad (35)$$

The quantities (34), (35) are spatially constant, when taken for the solutions to (26) inside the central electrode and the external leads, respectively. However, the boundary conditions (27) generally destroy the conservation of \mathcal{E} through the interfaces, in contrast to the conservation of the supercurrent. Therefore, \mathcal{E}_n and \mathcal{E} can substantially differ from each other.

After introducing the function $t(x) = f^2(x)$, the quantity \mathcal{E}_n for the central electrode can be expressed via $t_\pm = f_\pm^2$. To this end, one takes $x = (l/2) - 0$ in (34) and excludes the derivatives making use of (28) and the first equation in (27):

$$\mathcal{E}_n = \left[-1 + (g_{n,\delta} + g_\ell)^2 \right] t_- + g_\ell^2 t_+ - 2g_\ell (g_\ell + g_{n,\delta}) \cos \chi \sqrt{t_- t_+} - \frac{1}{2} t_-^2. \quad (36)$$

The first GL equation in (26) can be analytically solved under the conditions $f_- \sim g_\ell f_+ \ll 1$ and $g_{n,\delta} \lesssim g_\ell$, which in particular allow one to disregard the cubic term, as compared to the linear one:

$$\frac{d^2 f}{dx^2} - \frac{i^2}{f^3} - f = 0, \quad |x| < l/2. \quad (37)$$

The solution to (37) can be represented as

$$f(x) = \sqrt{t_1 \cosh^2 x - t_2 \sinh^2 x}, \quad (38)$$

where the parameters $t_1 \geq 0$ and $t_2 \leq 0$ satisfy

$$t_1 t_2 = -i^2, \quad t_1 + t_2 = -\mathcal{E}_n. \quad (39)$$

The order parameter absolute value has the maximums f_- inside the central lead at its end faces $x = \pm l/2$ and the minimum f_+ at its center $x = 0$. As can be confirmed (see (42)), under the conditions in question the quantity f_- is of the same order of smallness as $g_\ell f_+$ and, therefore, can satisfy the relation $f_- \gg 2g_\ell (g_\ell + g_{n,\delta}) f_+$ that reduces the expression (36) for \mathcal{E}_n to the following simplified form

$$\mathcal{E}_n = -t_- + g_\ell^2 t_+. \quad (40)$$

The equalities (38)-(40) and (28) lead to the following system of equations

$$\begin{aligned} t_1 t_2 &= -g_\ell^2 t_- t_+ \sin^2 \chi_r, \\ t_1 + t_2 &= t_- - g_\ell^2 t_+, \\ t_- &= t_1 \cosh^2 \frac{l}{2} - t_2 \sinh^2 \frac{l}{2}. \end{aligned} \quad (41)$$

Here t_- and $t_{1,2}$ are on the order of $g_\ell^2 t_+$, with the higher order terms disregarded.

One finds two solutions to equations (41) that are of the form

$$f_{-, \pm} = g_\ell f_+ \coth l \left[\cos \chi \pm \sqrt{\cos^2 \chi - \tanh^2 l} \right], \quad (42)$$

$$t_{1, \pm} = \frac{1}{2} g_\ell^2 t_+ \left\{ -2 + \left(1 + \coth^2 \frac{l}{2} \right) \cos \chi \left[\cos \chi \pm \sqrt{\cos^2 \chi - \tanh^2 l} \right] \right\}, \quad (43)$$

$$t_{2, \pm} = \frac{1}{2} g_\ell^2 t_+ \left\{ -2 + \left(1 + \tanh^2 \frac{l}{2} \right) \cos \chi \left[\cos \chi \pm \sqrt{\cos^2 \chi - \tanh^2 l} \right] \right\}, \quad (44)$$

and occur under the condition

$$|\chi| \leq \chi_{\max}(l) = \arccos \tanh l. \quad (45)$$

In the same framework f_∞ coincides with its currentless value (33) and t_+ is taken in (42)-(44) in the zeroth order approximation in g_ℓ , i.e., $t_+^{(0)} = \frac{b_n |a|}{b a_n}$ with the normalization used.

As seen in (42), the first solution $f_{-,+}(\chi, l)$ for f_- taken at the end face has its maximum at $\chi = 0$ and minimum at $\chi = \pm \chi_{\max}(l)$, while the second solution $f_{-,-}(\chi, l)$ for f_- has its maximum at $\chi = \chi_{\max}(l)$ and minimum at $\chi = 0$:

$$f_{-,+}(0, l) = g_\ell \coth \frac{l}{2} \left(\frac{b_n |a|}{b a_n} \right)^{1/2}, \quad (46)$$

$$f_{-,-}(0, l) = g_\ell \tanh \frac{l}{2} \left(\frac{b_n |a|}{b a_n} \right)^{1/2}, \quad (47)$$

$$f_{-, \pm}(\chi_{\max}(l), l) = g_\ell \left(\frac{b_n |a|}{b a_n} \right)^{1/2}. \quad (48)$$

The quantity $f_{-, \pm}(\chi_{\max}(l), l)$ does not depend on l within the approximation used, and the vanishing value $f_{-,-}(0, l) \rightarrow 0$ in the limit $l \rightarrow 0$ agrees with the exact result for the second solution at $\chi = 0$ (see Supplemental Material in [40]).

Substituting the maximal order parameter value (46) in the presumed condition $f_- \ll 1$, one finds that the first solution in (38), (42)-(44), taken at $\cos \chi \sim 1$, is justified when the length of the central lead is not too small: $l \gg 2g_\ell \left(\frac{b_n |a|}{b a_n} \right)^{1/2}$. For the parameter set used in plotting the figures, one gets $l \gg 0.02$. The first solution at sufficiently small l has been considered in Supplemental Material in [40]. One notes that the results of this section can be applied at any l to the second solution, as well as to the first one in a vicinity of $\chi = \chi_{\max}(l)$.

For the absolute order parameter value at the center of the normal metal lead $f(x=0, \chi, l) \equiv f_1(\chi, l)$, one finds from (38) and (43):

$$f_{1,+}(0, l) = \frac{g_\ell}{\sinh \frac{l}{2}} \left(\frac{b_n |a|}{b a_n} \right)^{1/2}, \quad (49)$$

$$f_{1,-}(0, l) = 0, \quad (50)$$

$$f_{1, \pm}(\chi_{\max}(l), l) = \frac{g_\ell}{\sqrt{\cosh l}} \left(\frac{b_n |a|}{b a_n} \right)^{1/2}. \quad (51)$$

The vanishing second solution in (50) at the center of the lead at $\chi = 0$ makes possible phase-slip processes at $\phi = \pi$, and at arbitrary l , in agreement with earlier results [38, 43]. The corresponding phase incursion is $\varphi = \pi$ and the supercurrent vanishes under such a condition. As seen in (28), the phase incursion can differ from zero in the limit $i \rightarrow 0$ only if the order parameter $f(x) \geq 0$ takes its minimum value $f = 0$ somewhere inside the central electrode. This is the case at $x = 0$.

One obtains from (28) and the solutions (38), (42) - (44) the following expression for the phase incursion φ :

$$\varphi_{\pm}(\chi, l) = \text{sgn}(\sin \chi) \arccos \left[\cosh l \left(\sin^2 \chi \pm \cos \chi \sqrt{\cos^2 \chi - \tanh^2 l} \right) \right]. \quad (52)$$

One gets $\varphi_+(0, l) = 0$ from (52) for the first solution and $\varphi_-(0, l) = \pi$ for the second one and $\varphi_{\pm}(\chi_{\max}(l), l) = \arccos(1/\cosh l)$, where $\chi_{\max}(l)$ is defined in (45). Therefore, there are two possible values 0 and π of the phase incursion φ in currentless states of the double junctions in question, as have been earlier identified in Refs. [42] and [43].

For the external phase difference, which satisfies the relation $\phi(\chi, l) = 2\chi + \varphi_{\pm}(\chi, l)$, one finds

$$\sin \phi_{\pm}(\chi, l) = \left[\cos \chi \pm \sqrt{\cos^2 \chi - \tanh^2 l} \right] \cosh l \sin \chi. \quad (53)$$

For $\phi_*(l) \equiv \phi(\chi_{\max}(l), l)$ one gets from (53):

$$\phi_*(l) = \frac{\pi}{2} + \arcsin(1/\cosh l). \quad (54)$$

Thus, for the double tunnel junction considered, it follows from (28), (42) and (53) the conventional sinusoidal current-phase relation with respect to the external phase difference:

$$i = \frac{g_{\ell}^2}{\sinh l} t_+ \sin \phi. \quad (55)$$

Deviations of the dashed curves from solid ones in Figs. 2 - 4 demonstrate a reasonable accuracy of the analytical results of this subsection with respect to the corresponding results of exact numerical calculations. Although, the accuracy of the phase relations (52)-(54) is noticeably better as compared with the expressions (38), (42)-(44) obtained for the absolute value of the order parameter within the same approximation. One notes that the coupling constants have canceled out in (52)-(54), as distinct from (42)-(44).

4. INTERNAL PHASE DIFFERENCES IN SYMMETRIC SISIS DOUBLE JUNCTIONS

4.1. Preliminary Remarks

As was demonstrated in the preceding section for SINIS double junctions, the Josephson coupling associated with the phase-dependent bilinear part of free energy $-2g_J |\Psi_-| |\Psi_+| \cos \chi$ (see (1)) is responsible for the supercurrent on condition that $g_{\ell} \cos \chi > 0$. This is necessary for a nonzero order parameter $|\Psi_-|$ on the normal metal interface side to be induced in the presence of $|\Psi_+|$ on the opposite superconducting side of a thin interface. As a result, for superconductivity to be proximity-induced over zero junctions ($g_J > 0$) in the normal metal electrode, the internal phase difference χ must be confined within a substantially reduced range $|\chi| \leq \chi_{\max}(l) < \frac{\pi}{2}$ (modulo 2π). Outside of that range the Josephson coupling prevents superconductivity from showing up in the normal metal lead, within the model discussed. The quantity $\chi_{\max}(l)$ is less than $\frac{\pi}{2}$ due to the effect of the current-induced phase incursion along the central lead. In the SISIS systems with the central-electrode length of a mesoscopic size, the effect of the phase incursion is usually negligibly small except for an immediate vicinity of $|\chi| = \pi/2$.

Unlike SINIS double junctions, all three electrodes in SISIS heterostructures possess identical original superconducting properties. Proximity and pair-breaking effects are not necessary in the latter case for producing the supercurrent itself, although they can noticeably modify its properties under certain conditions. For zero junctions, the phase-dependent part of the Josephson interface free energy $-2g_J |\Psi_-| |\Psi_+| \cos \chi$ shifts the energies of the states with $|\chi| < \pi/2$ and $\pi/2 < |\chi| < \pi$ down and up, respectively. In other words, the Josephson coupling is responsible for a superconductivity enhancement under the condition $|\chi| < \pi/2$, while for $\pi/2 < |\chi| < \pi$ it has pair breaking character. This results in the presence of lower and higher energy modes in the system.

When the central electrode's length L substantially exceeds the superconductor coherence length, the internal phase difference χ can generally take any value in SISIS superconducting double junctions. However, with decreasing length L , a difference between the energies of the two types of modes increases, and the pair breaking of the Josephson origin can play a crucial role in destroying the higher energy modes, when L is less than a phase dependent critical value [20]. This results in a reduced length-dependent range of variations of χ . In particular, as will be seen below, the lower energy state with $\chi_1 = \chi_2 = 0$ occurs at an arbitrary L , while the higher energy equilibrium state with

$\chi_1 = \chi_2 = \pi$ exists only for L exceeding a critical length L_π . The formation of the proximity-reduced range of the internal phase difference in SISIS double junctions also depends on the Josephson coupling strength. In the limit of vanishing strength, the range agrees with the known result, which states that superconductivity is completely destroyed in a metal film sandwiched between two impenetrable pair breaking walls when the film's thickness L is less than its critical (phase-independent) value [54, 77, 102, 103].

On the other hand, the Josephson current is, generally speaking, not uniquely defined at a fixed phase difference ϕ between the external leads, when a sufficiently wide range of $\chi_{1,2}$ is allowed. Consider, for example, the relation $\phi = \chi_1 + \chi_2$ assuming the phase incursion over the central lead to be negligibly small. For symmetric double junctions one can take $\chi_1 = \chi_2 + 2\pi n$ with integer n , that results in $\chi_1 = \frac{\phi}{2} + \pi n$. Therefore, after switching from $\chi_{1,2}$ to ϕ , the 2π -periodic current-phase relation $j(\chi_1)$ for a single junction is transformed into two different 4π -periodic modes $j(\frac{\phi}{2})$ and $j(\frac{\phi}{2} + \pi)$, with respect to ϕ . The change of ϕ by 2π , caused by the variations of both $\chi_{1,2}$ by π , results in the supercurrent sign change for each separate mode. Although, if the same change $\phi \rightarrow \phi + 2\pi$ occurs when only one of $\chi_{1,2}$ varies by 2π , the current remains unchanged. Thus, the supercurrent is a double-valued function of ϕ that can be verified, when $\chi_{1,2}$ are independently controlled in experiments.

However, if the external phase difference ϕ is experimentally controlled, $\chi_{1,2}$ can take on the most preferable equilibrium values. The first mode $j(\frac{\phi}{2})$ is energetically favorable under the condition $(4n - 1)\pi \leq \phi \leq (4n + 1)\pi$, while the second mode $j(\frac{\phi}{2} + \pi)$ is favorable at $(4n + 1)\pi \leq \phi \leq (4n + 3)\pi$. Therefore, the two 4π -periodic states get interchanged when the external phase ϕ changes by 2π , if disregarding possible ‘‘undercooling’’ or ‘‘overheating’’ of the states during the transition. Such a regime of interchanging modes is characterized by a 2π -periodic sawtooth-like current-phase relation with discontinuities at $\phi = (2n + 1)\pi$ [19, 20, 104], as shown below in the curve 1 in the right panel of Fig. 7. It is a characteristic feature of conventional superconducting double junctions, considered both in this and the preceding sections, that a potential 4π -periodic current-phase dependence, related to the external phase difference ϕ , gets, for one reason or another, broken and transformed into a 2π -periodic behavior. This differs clearly from the real 4π -periodic supercurrent through Josephson junctions involving Majorana fermions [105–110].

A sharp change of the supercurrent, that takes place in this regime in immediate vicinities of $\phi_n = (2n + 1)\pi$, can occur continuously and involve the current-carrying asymmetric states. In the tunneling limit, the symmetry $j(\pi - \chi) = j(\chi)$ allows one to get the value $\phi = \chi_1 + \chi_2 = \pi$ with $\chi_2 = \pi - \chi_1$ at all possible χ_1 and, therefore, at any admissible value of the supercurrent $|j| \leq j_c$. For sufficiently small central electrode length, the proximity effects reduce the range of $\chi_{1,2}$ and the order parameter values in the central lead. As a result, the regime of interchanging modes is destroyed and the conventional smooth current-phase relation $j(\phi)$ is restored at all ϕ in this limit [20]. The abrupt change, produced by a competition of the doubled condensate states at given ϕ , can also be partially smeared out by fluctuations, small junction asymmetries etc [19].

In the limit of small L , the double Josephson junction can be considered as an effective single junction with a thin interface involving the central region. Although this is a specific interface, where only a sequential tunneling takes place, while a direct one is forbidden within the model in question, the single-junction regular phase dependence $j(\phi)$ at all ϕ occurs in this limit. The experimental data support this issue [9]. The microscopic studies revealed the conventional single junction behavior at a very small L , but without taking the regime of interchanging modes at the larger L into account [10, 13, 15, 44]. The proximity effects at $L \ll \xi$ have been known to be responsible for a pronounced order parameter's phase-dependence in the central lead.

A theory of the proximity-influenced regime of interchanging modes and of the behavior of internal phase differences in symmetric SISIS double Josephson junctions considered below, was developed in Ref. [20] within the GL approach based on the interface boundary conditions discussed in Sec. 2.

4.2. Model and Basic Equations

Consider a symmetric SISIS double junction, shown in Fig. 5, that contains two identical thin interfaces at a distance L , connected by the central superconducting electrode made of the same superconducting material as the external leads. Similar to Secs. 2 - 3, a comparatively small interface thickness is assumed for defining it to be zero within the GL theory. The length of the external leads is supposed to be large, significantly exceeding the coherence length $\xi(T)$. The one-dimensional spatial dependence of the order parameter considered below occurs, for example, when the transverse dimensions of all three electrodes are significantly less than $\xi(T)$ as well as the magnetic penetration depth.

The system's free energy incorporates the interface and bulk contributions $\mathcal{F} = \sum \mathcal{F}_p + \mathcal{F}_{\frac{L}{2}}^{\text{int}} + \mathcal{F}_{-\frac{L}{2}}^{\text{int}}$, where $p = 1, 2$ correspond to the external electrodes and $p = 3$ refers to the central lead. The bulk free energies per unit area of the

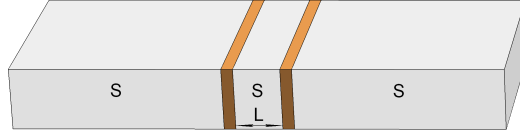


Figure 5: Schematic diagram of the double SISIS junction. Adopted from Ref. [20].

cross section are

$$\mathcal{F}_p = \int_{\mathcal{C}_p} dX \left[K \left| \frac{d}{dX} \Psi(X) \right|^2 + a |\Psi(X)|^2 + \frac{b}{2} |\Psi(X)|^4 \right]. \quad (56)$$

The integration periods \mathcal{C}_p for $p = 1, 2, 3$ are taken to be $(-\infty, -L/2)$, $(L/2, \infty)$ and $(-L/2, L/2)$, respectively.

For each of two interfaces placed at $X = \pm L/2$, the interfacial free energy per unit area is, in accordance with (5),

$$\mathcal{F}_{\pm \frac{L}{2}}^{\text{int}} = g_J \left| \Psi_{\pm \frac{L}{2}+} - \Psi_{\pm \frac{L}{2}-} \right|^2 + g \left(\left| \Psi_{\pm \frac{L}{2}+} \right|^2 + \left| \Psi_{\pm \frac{L}{2}-} \right|^2 \right). \quad (57)$$

For 0-junctions considered below the Josephson coupling constant $g_J > 0$. The parameter $g > 0$ describes the strength of the surface pair breaking.

The GL equation, applied to the normalized absolute value of the superconductor order parameter $\Psi = (|a|/b)^{1/2} f e^{i\alpha}$, takes the form

$$\frac{d^2 f}{dx^2} - \frac{i^2}{f^3} + f - f^3 = 0, \quad (58)$$

where $x = X/\xi(T)$, $\xi(T) = (K/|a|)^{1/2}$ and the dimensionless current density is $i = \frac{2}{3\sqrt{3}}(j/j_{\text{dp}})$, where $j_{\text{dp}} = (8|e||a|^{3/2}K^{1/2})/(3\sqrt{3}\hbar b)$ is the depairing current deep inside the external superconducting leads.

The boundary conditions, that follow from (56) and (57), are in agreement with (6). After introducing the dimensionless real quantities, the conditions at $x = l/2$, where $l = L/\xi(T)$, can be written as

$$\left(\frac{df}{dx} \right)_{l/2\pm 0} = \pm (g_\delta + g_\ell) f_{l/2\pm 0} \mp g_\ell \cos \chi f_{l/2\mp 0}, \quad (59)$$

$$i = -f^2 \left(\frac{d\alpha}{dx} + \frac{2\pi\xi(T)}{\Phi_0} A \right) = g_\ell f_{l/2-0} f_{l/2+0} \sin \chi. \quad (60)$$

Here $\chi = \alpha(\frac{l}{2} - 0) - \alpha(\frac{l}{2} + 0)$, $\Phi_0 = \frac{\pi\hbar c}{|e|}$ and the dimensionless coupling constants are introduced $g_\ell = g_J \xi(T)/K$, $g_\delta = g\xi(T)/K$.

As this follows from the boundary conditions (59) and the conservation of the supercurrent (60), the order parameter values $f_{l/2\pm 0}$ on opposite sides of an interface between identical superconductors can generally differ from one another. This is usually not the case in a single symmetric Josephson junction, where $f(x)$ is continuous across a thin interface. However, the condensate density can be noticeably weakened by pair breaking interfacial effects on both ends of the central lead of mesoscopic length of the double junction. The resulting phase dependent jump $f_{l/2+0} - f_{l/2-0} > 0$ plays an important role allowing superconductivity to survive in the central lead with a small length $l \ll 1$ despite the interface pair breaking. The fallacious continuity of $f(x)$ across thin interfaces in double Josephson junctions is a characteristic feature of earlier theories that used the flawed boundary conditions for the order parameter within the GL approach [111–113]. As follows from Subsec. 2.2.3, those models disagree with the microscopic results near T_c .

A number of solutions to equation (58) were found that satisfy the asymptotic conditions in the external electrodes and the boundary conditions at $x = \pm l/2$ (see Appendix A in Ref. [20] for details). The solutions that possess the extrema only at $x = 0, \pm l/2, \pm\infty$, or, when possible, only at $x = \pm l/2, \pm\infty$ are assumed to have preferable energies. The symmetric solutions $f(x) = f(-x)$ with the internal phase differences $\chi_1 = \chi_2 + 2\pi n = \chi$, exist in most cases considered below, with the exception of close vicinities of $\phi_n = (2n + 1)\pi$, where the asymmetric behavior can take place.

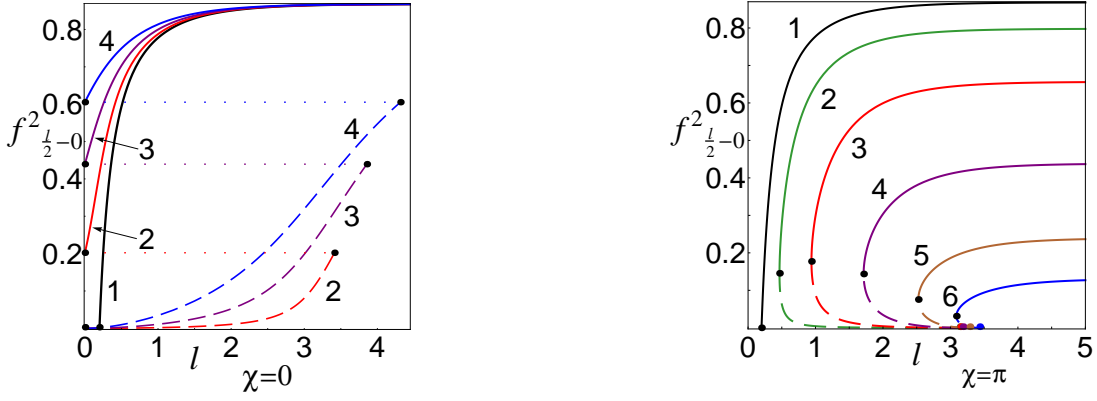


Figure 6: $f_{l/2-0}^2$ as a function of l at $\chi = 0$ (left panel) and $\chi = \pi$ (right panel). Solid curves correspond to the energetically preferable states. *Left panel:* $\chi = 0$, $g_\delta = 0.1$ and (1) $g_\ell = 0$ (2) $g_\ell = 0.1$ (3) $g_\ell = 0.3$, and (4) $g_\ell = 0.8$. *Right panel:* $\chi = \pi$, $g_\delta = 0.1$ and (1) $g_\ell = 0$ (2) $g_\ell = 0.03$ (3) $g_\ell = 0.1$, (4) $g_\ell = 0.25$, (5) $g_\ell = 0.5$, and (6) $g_\ell = 0.8$. Adopted from Ref. [20].

4.3. Currentless States at $\chi = 0, \pi$

The double junction's states can be described analytically in the absence of the supercurrent, i.e., at $\chi = \pi n$ [20]. Fig. 6 shows the dependence of the quantity $f_{l/2-0}^2(\chi, g_\ell, g_\delta)$, taken at the end side of the central lead, on its dimensionless length l at $\chi = 0$ (the left panel) and $\chi = \pi$ (the right panel), calculated with $g_\delta = 0.1$ at various g_ℓ . The solid curves correspond to energetically preferable solutions, while the dashed curves describe metastable states.

The curves 1 in both panels in Fig. 6 are identical due to vanishing dependence on the phase difference for an impenetrable wall ($g_\ell = 0$). As known, superconductivity is destroyed in the sample placed between two impenetrable pair breaking walls with decreasing distance L between them, and the transition to the normal metal state occurs at $L = 2\xi(T) \arctan g_\delta$ [54, 77, 103]. For $g_\delta = 0.1$ one gets from here $l = 0.199$. However, as seen in the solid curves 2-4 in the left panel of Fig. 6, the nonzero minimum of the quantity $f_{l/2-0}^2$ is at $l = 0$ in the presence of a finite interface transparency ($g_\ell > 0$), but not in the limit $g_\ell \rightarrow 0$ at $g_\delta \neq 0$. Therefore, despite the surface pair breaking, the finite interface transparency allows the superconducting state at $\chi = 0$ to exist in the central electrode at any small value of its length.

According to the boundary condition $(df/dx)_{(l/2)-0} = -(g_\delta + g_\ell)f_{(l/2)-0} + g_\ell f_{(l/2)+0}$ taken at $\chi = 0$, the order parameter derivative is negative under the condition $f_{(l/2)-0} > g_\ell f_{(l/2)+0}/(g_\delta + g_\ell)$ and, therefore, $f(x)$ increases, when $x > 0$ goes down to $x = 0$. The corresponding solutions are shown in the solid curves 2 - 4 in the left panel of Fig. 6. The derivative $(df/dx)_{(l/2)-0}$ vanishes at the end face of the central lead, if the equality $f_{(l/2)-0} = g_\ell f_{(l/2)+0}/(g_\delta + g_\ell)$ holds. The dashed curves in the left panel of Fig. 6 correspond to the solution of a different type, for which the order parameter derivative is positive $(df/dx)_{(l/2)-0} > 0$ and $f(x)$ decreases with decreasing x inside the central lead vanishing at $x = 0$. This is a metastable solution that takes smaller order parameter values and satisfies the relation $f_{(l/2)-0} < g_\ell f_{(l/2)+0}/(g_\delta + g_\ell)$.

As distinct from the case $\chi = 0$, both terms on the right-hand side of the boundary conditions (59) have negative sign at $\chi = \pi$, as well as at all $\pi/2 < |\chi| \leq \pi$. For this reason, the sign of the order parameter derivative at $\chi = \pi$ is negative in the central electrode irrespective of the relation between $f_{(l/2)-0}$ and $f_{(l/2)+0}$. In this case the condensate density at $x > 0$ always decreases the nearer one gets to the interface. Under such conditions, the state with $\chi = \pi$ exists only if the central electrode's length l exceeds the critical value $l_\pi(g_\ell, g_\delta)$. However, in contrast to what takes place at $g_\ell \equiv 0$, a disappearance of the equilibrium state with $\chi = \pi$ at $l < l_\pi(g_\ell, g_\delta)$ and $g_\ell \neq 0$ is not associated with a system's transition to the normal metal state.

Since the system involves distant superconducting regions of the external electrodes, the transition to the normal metal state cannot be induced by the interfacial pair breaking which is confined by the scale $\lesssim \xi(T)$. Also, the central electrode cannot individually be in the normal metal state ($f(x) = 0$ at $|x| < l/2 - 0$) once $g_\ell \neq 0$. In this case the boundary condition $(df/dx)_{(l/2)-0} = -(g_\delta + g_\ell)f_{(l/2)-0} - g_\ell f_{(l/2)+0}$ at $x = l/2 - 0$ and $\chi = \pi$ would result in $f_{(l/2)+0} = 0$. One would also obtain $(df/dx)_{(l/2)+0} = 0$ from the boundary condition on the opposite side of the interface. This would mean the normal metal state of the external leads, which is not possible as stated above. Therefore, superconductivity does exist under the conditions $l < l_\pi(g_\ell, g_\delta)$ and $g_\ell \neq 0$ due to the proximity to the external superconducting leads, while the value $\chi = \pi$ cannot be the equilibrium value of χ . Similar effects, that

reduce the range of variation of χ , take place for all $\pi/2 < |\chi| \leq \pi$ with the phase-dependent critical length $l_\chi(g_\ell, g_\delta)$.

The dashed curves in the right panel of Fig. 6 describe metastable solutions at $\chi = \pi$. They appear within the range $l_\pi(g_\ell, g_\delta) < l < l_{ps}(g_\ell, g_\delta)$ being of the same type as the energetically preferable solutions. At $l = l_{ps}(g_\ell, g_\delta)$, the metastable phase-slip centers, where $f_{\pm}(l_{ps}/2-0) = 0$, appear at the central lead's end interfaces. The length l_{ps} takes on its minimum value $l_{ps}(g_\ell \rightarrow 0, g_\delta) = \pi$ in the tunneling limit. The points with coordinates $l = l_{ps}(g_\ell, g_\delta)$ and $f_{l/2-0} = 0$ are marked in the right panel of Fig. 6.

The numerical study of the solutions shows that the left and right panels of Fig. 6 depict the two basic types of mapping functions $f_{l/2-0}^2$. One type is transformed into another with χ at some distance below $\chi = \pi/2$.

4.4. Central Electrode with a Small Length $l \ll 1$

In the limit of small central electrode's length l at a given phase difference χ , the order parameter absolute values on opposite interface sides are linked by a relation that follows from the boundary conditions and corresponds to approximately vanishing order parameter derivative in the central region [20]. As seen from the boundary conditions (59), the derivative $(df/dx)_{l/2-0}$ vanishes, if, similar to (30), $\cos \chi > 0$ and the order parameter absolute values satisfy the relation:

$$f_{l/2-0} = \frac{g_\ell \cos \chi}{g_\ell + g_\delta} f_{l/2+0}. \quad (61)$$

This demonstrates that, in the limit of small length l , a superconducting state survives in the central electrode under the condition $\cos \chi > 0$ ($g_\ell > 0$). The pair breaking effects of the Josephson origin prohibit in this limit the equilibrium values of internal phase differences with $\cos \chi < 0$.

Internal phase differences that satisfy the condition $\cos \chi > 0$, form allowed bands $-\pi/2 + 2\pi n < \chi < \pi/2 + 2\pi n$ separated by the forbidden gaps. After switching over to the external phase difference ϕ and disregarding the phase incursion over the central lead, one obtains the same bands for the argument $\frac{\phi}{2}$ of the first mode and for the argument $\frac{\phi}{2} + \pi$ of the second mode. Therefore, the functions $\cos \chi$ and $\sin \chi$ correspond here to $\cos \frac{\phi}{2}$ and $\sin \frac{\phi}{2}$, if $(4n-1)\pi \leq \phi \leq (4n+1)\pi$, and to $\cos(\frac{\phi}{2} + \pi) = -\cos \frac{\phi}{2}$ and $-\sin \frac{\phi}{2}$ in the case $(4n+1)\pi \leq \phi \leq (4n+3)\pi$. Thus, one obtains from (61) at any value of ϕ

$$f_{l/2-0} = \frac{g_\ell |\cos \frac{\phi}{2}|}{g_\delta + g_\ell} f_{l/2+0}, \quad (62)$$

$$i = g_\ell^{\text{eff}} f_{l/2+0}^2 \sin \phi, \quad g_\ell^{\text{eff}} = \frac{g_\ell^2}{2(g_\delta + g_\ell)}, \quad (63)$$

where the right hand side in (60) has been used in (63).

Thus, in the limit $l \ll 1$, the allowed bands from both modes for the external phase difference ϕ are adjoined with no overlapping portions and with no gaps. This leads to the single-valued dependence on ϕ of the quantities considered, at all values of ϕ . However, while the higher energy mode is completely destroyed in the limit of very small l due to the proximity reduced range of the internal phase differences, it is present to the full extent at comparatively large l . The total annihilation of the condensate states' doubling at any given ϕ and the expression (63) for the supercurrent demonstrate that the double junction behavior in the limit $l \rightarrow 0$ is transformed to that of a symmetric single junction with the effective Josephson coupling constant g_ℓ^{eff} .

The boundary condition for a single symmetric Josephson junction [72] follows from (59) under the condition $f_{l/2-0} = f_{l/2+0}$ that allows one to exclude the order parameter taken at the internal interface side:

$$\left(\frac{df}{dx}\right)_{l/2+0} = (g_\delta + 2g_\ell \sin^2 \frac{\chi}{2}) f_{l/2+0}. \quad (64)$$

For the double junctions with $l \ll 1$, one can exclude, based on (62), the internal value $f_{l/2-0}$ in (59) in favor of $f_{l/2+0}$ and obtain an approximate boundary condition of the same form as (64), but with the effective Josephson coupling constant g_ℓ^{eff} , defined in (63), and the effective interfacial pair breaking parameter

$$g_\delta^{\text{eff}} = \frac{g_\delta(g_\delta + 2g_\ell)}{g_\delta + g_\ell}. \quad (65)$$

In the limit $l \ll 1$, the proximity effects play a crucial role in establishing the conventional sinusoidal current-phase relation (63) in the SISIS double junction, if the sequential tunneling dominates the direct one in the system. This

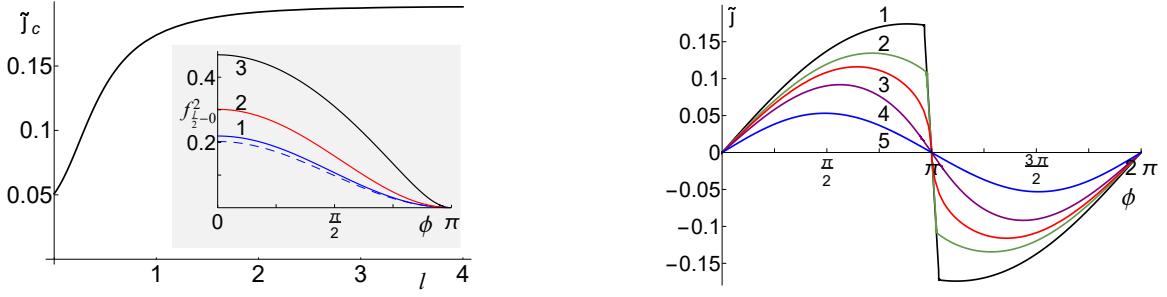


Figure 7: Left panel: Critical current as a function of l at $g_\ell = 0.1$, $g_\delta = 0.1$. Inset: The quantity $f_{l/2-0}(\phi)$ at (1) $l = 0.02$ (2) $l = 0.1$ (3) $l = 0.25$. Right panel: Current-phase relations $\tilde{j}(\phi)$ taken for $g_\ell = 0.1$, $g_\delta = 0.1$ and (1) $l = 1$ (2) $l = 0.5$ (3) $l = 0.38$ (4) $l = 0.25$ (5) $l = 0.02$. Adopted from Ref. [20].

is the proximity-induced phase dependent factor $|\cos \frac{\phi}{2}|$ on the right-hand side of (62), which is responsible in this case for the supercurrent (63) to decrease with increasing ϕ at $\pi/2 \leq \phi \leq \pi$. As discussed in Subsec. 22.3, in tunnel junctions $g_\ell \propto \mathcal{D}$, where \mathcal{D} is the interface transmission coefficient. Therefore one obtains from (63) $g_\ell^{\text{eff}} \propto \mathcal{D}^2$ under the condition $g_\delta \gg g_\ell$, and $g_\ell \propto \mathcal{D}$ in the opposite limit $g_\delta \ll g_\ell$, in agreement with the earlier microscopic results [10, 13, 44].

A pronounced suppression of the quantity $f_{l/2-0}$ in a close vicinity of $\phi = \pi$, that follows from (62), and the spatial uniformity of the supercurrent (60) result in a large gradient of the order-parameter phase. The numerical data show that a noticeable phase incursion over the central lead arises for this reason even at very small l and violates near $\phi = \pi$ the applicability of the approximation used. After switching over to χ , this results in no discernible modifications in (62) and (63), but the range of χ diminishes so that only values at a distance below $\chi = \pi/2$ are permitted at small l : $\chi(\phi) < \pi/2$ at $\phi = \pi$.

The inset in the left panel of Fig. 7 shows the phase dependence of order parameter squared $f_{l/2-0}^2$ at the end face of the central lead. The solid curves 1 - 3 correspond to the numerical results. The dashed curve depicts the analytical results, which follow from the right-hand side of (62) at $l = 0.02$ and deviates only by a few percent from the curve 1. However, the dashed curves at $l = 0.1$ and $l = 0.25$ (not shown) almost coincide with the one presented for $l = 0.02$ and, therefore, substantially deviate from the solid curves 2 and 3. In other words, the relation (62), which is justified at $l = 0.02$ for the chosen set of parameters, is, with increasing l , in contradiction with the careful numerical calculations already at $l = 0.1$ and $l = 0.25$. The origin of the discrepancy is that the right-hand side of (62), obtained in the limit of small l , does not depend on l as is justified by a negligibly weak dependence on l of the order parameter $f_{l/2+0}$ on the end face of the external lead.

The proximity-modified current-phase relation $\tilde{j}(\phi)$ is depicted at various l in the right panel of Fig. 7 for the normalized supercurrent $\tilde{j} = j/j_{\text{dp}}$ and the interfaces with $g_\ell = g_\delta = 0.1$. The supercurrent has been numerically evaluated, taking into account the phase incursion over the central lead, based on (60) and the consistent solutions of GL equations for the system (56), (57). A weakening of the regime of interchanging modes, taking place with decreasing l at $l = 1$ and $l = 0.5$, is seen in the curves 1 and 2 for the set of parameters chosen. The pair breaking effects below $l \approx 0.36$ fully destroy the asymmetric states and a noticeable abrupt change of the supercurrent in the vicinities of $\phi_n = (2n + 1)\pi$. However, the curve 5 for $l = 0.02$ within several percent coincides with the single junction sinusoidal current-phase dependence (63). Anharmonic contributions to $\tilde{j}(\phi)$ are seen in the curves 3 and 4. The dependence of the critical current on the central electrode's length l in the double junction is shown in the left main panel of Fig. 7.

Thus, in the SISIS double Josephson junctions with closely spaced interfaces, the range of the internal phase differences is gradually reduced with decreasing the length l of the central lead. The doubling of the current carrying condensate states taking place at any given ϕ , that occurs at $l \gtrsim 1$, is fully removed at very small l , when the regime of interchanging modes is destroyed and the conventional single junction expression (63) for the current-phase relation is established.

The work has been carried out within the state task of ISSP RAS.

-
- [1] B. Josephson, Possible new effects in superconductive tunnelling, Physics Letters **1**, 251 (1962).
 [2] B. D. Josephson, Coupled superconductors, Rev. Mod. Phys. **36**, 216 (1964).

- [3] B. D. Josephson, Supercurrents through barriers, *Adv. Phys.* **14**, 419 (1965).
- [4] D. W. Jillie, J. E. Lukens, and Y. H. Kao, Observation of interactions between two superconducting phase-slip centers, *Phys. Rev. Lett.* **38**, 915 (1977).
- [5] J. B. Hansen and P. E. Lindelof, Static and dynamic interactions between Josephson junctions, *Rev. Mod. Phys.* **56**, 431 (1984).
- [6] A. Jain, K. Likharev, J. Lukens, and J. Sauvageau, Mutual phase-locking in Josephson junction arrays, *Physics Reports* **109**, 309 (1984).
- [7] G. W. Frank, A. S. Deakin, M. A. H. Nerenberg, and J. A. Blackburn, Subharmonic locking in Josephson weak links, *Phys. Rev. B* **35**, 3138 (1987).
- [8] H. J. T. Smith and M. Dion, Closely coupled superconducting microbridges, *Phys. Rev. B* **42**, 206 (1990).
- [9] I. Nevirkovets, J. Evetts, and M. Blamire, Transition from single junction to double junction behaviour in SISIS-type Nb-based devices, *Physics Letters A* **187**, 119 (1994).
- [10] M. Kupriyanov, A. Brinkman, A. Golubov, M. Siegel, and H. Rogalla, Double-barrier Josephson structures as the novel elements for superconducting large-scale integrated circuits, *Physica C: Superconductivity* **326**, 16 (1999).
- [11] E. Goldobin and A. V. Ustinov, Current locking in magnetically coupled long Josephson junctions, *Phys. Rev. B* **59**, 11532 (1999).
- [12] I. P. Nevirkovets and S. E. Shafranjuk, Resonant Josephson tunneling in $s - i - s'$ -i-s multilayered devices, *Phys. Rev. B* **59**, 1311 (1999).
- [13] A. Brinkman and A. A. Golubov, Coherence effects in double-barrier Josephson junctions, *Phys. Rev. B* **61**, 11297 (2000).
- [14] A. Brinkman, D. Cassel, A. A. Golubov, M. Y. Kupriyanov, M. Siegel, and H. Rogalla, Double-barrier Josephson junctions: theory and experiment, *IEEE Transactions on Applied Superconductivity* **11**, 1146 (2001).
- [15] H. Ishikawa, S. Kurihara, and Y. Enomoto, Resonant states and currents in superconducting multilayers, *Physica C: Superconductivity* **350**, 62 (2001).
- [16] A. Brinkman, A. A. Golubov, H. Rogalla, F. K. Wilhelm, and M. Y. Kupriyanov, Microscopic nonequilibrium theory of double-barrier Josephson junctions, *Phys. Rev. B* **68**, 224513 (2003).
- [17] M. G. Blamire, Multiple-barrier and nanoscale superconducting devices, *Superconductor Science and Technology* **19**, S132 (2006).
- [18] L. Machura, J. Spiechowicz, M. Kostur, and J. Luczka, Two coupled Josephson junctions: dc voltage controlled by biharmonic current, *Journal of Physics: Condensed Matter* **24**, 085702 (2012).
- [19] J. A. Ouassou and J. Linder, Spin-switch Josephson junctions with magnetically tunable $\sin(\delta\varphi/n)$ current-phase relation, *Phys. Rev. B* **96**, 064516 (2017).
- [20] Y. S. Barash, Proximity-reduced range of internal phase differences in double Josephson junctions with closely spaced interfaces, *Phys. Rev. B* **97**, 224509 (2018).
- [21] S. V. Bakurskiy, A. A. Neilo, N. V. Klenov, I. I. Soloviev, and M. Y. Kupriyanov, Dynamic properties of asymmetric double Josephson junction stack with quasiparticle imbalance, *Nanotechnology* **30**, 324004 (2019).
- [22] P. G. de Gennes, Boundary effects in superconductors, *Rev. Mod. Phys.* **36**, 225 (1964).
- [23] K. K. Likharev, Superconducting weak links, *Rev. Mod. Phys.* **51**, 101 (1979).
- [24] W. Belzig, F. K. Wilhelm, C. Bruder, G. Schön, and A. D. Zaikin, Quasiclassical Green's function approach to mesoscopic superconductivity, *Superlattices and Microstructures* **25**, 1251 (1999).
- [25] T. M. Klapwijk, Proximity effect from an Andreev perspective, *Journal of Superconductivity* **17**, 593 (2004).
- [26] A. A. Golubov, M. Y. Kupriyanov, and E. Il'ichev, The current-phase relation in Josephson junctions, *Rev. Mod. Phys.* **76**, 411 (2004).
- [27] V. T. Petrashov, V. N. Antonov, P. Delsing, and T. Claeson, Phase controlled conductance of mesoscopic structures with superconducting "mirrors", *Phys. Rev. Lett.* **74**, 5268 (1995).
- [28] S. Guéron, H. Pothier, N. O. Birge, D. Esteve, and M. H. Devoret, Superconducting proximity effect probed on a mesoscopic length scale, *Phys. Rev. Lett.* **77**, 3025 (1996).
- [29] D. Balashov, F.-I. Buchholz, H. Schulze, M. I. Khabipov, W. Kessel, and J. Niemeyer, Superconductor-insulator-normal-conductor-insulator-superconductor process development for integrated circuit applications, *Superconductor Science and Technology* **11**, 1401 (1998).
- [30] P. Dubos, H. Courtois, B. Pannetier, F. K. Wilhelm, A. D. Zaikin, and G. Schön, Josephson critical current in a long mesoscopic S-N-S junction, *Phys. Rev. B* **63**, 064502 (2001).
- [31] W. Belzig, R. Shaikhaidarov, V. V. Petrashov, and Y. V. Nazarov, Negative magnetoresistance in Andreev interferometers, *Phys. Rev. B* **66**, 220505 (2002).
- [32] H. le Sueur, P. Joyez, H. Pothier, C. Urbina, and D. Esteve, Phase controlled superconducting proximity effect probed by tunneling spectroscopy, *Phys. Rev. Lett.* **100**, 197002 (2008).
- [33] F. Giazotto, J. T. Peltonen, M. Meschke, and J. P. Pekola, Superconducting quantum interference proximity transistor, *Nature Physics* **6**, 254 (2010).
- [34] M. Meschke, J. T. Peltonen, J. P. Pekola, and F. Giazotto, Tunnel spectroscopy of a proximity Josephson junction, *Phys. Rev. B* **84**, 214514 (2011).
- [35] F. Giazotto and F. Taddei, Hybrid superconducting quantum magnetometer, *Phys. Rev. B* **84**, 214502 (2011).
- [36] A. Ronzani, C. Altimiras, and F. Giazotto, Highly sensitive superconducting quantum-interference proximity transistor, *Phys. Rev. Applied* **2**, 024005 (2014).
- [37] S. D'Ambrosio, M. Meissner, C. Blanc, A. Ronzani, and F. Giazotto, Normal metal tunnel junction-based superconducting

- quantum interference proximity transistor, *Applied Physics Letters* **107**, 113110 (2015).
- [38] A. Ronzani, S. D'Ambrosio, P. Virtanen, F. Giazotto, and C. Altimiras, Phase-driven collapse of the Cooper condensate in a nanosized superconductor, *Phys. Rev. B* **96**, 214517 (2017).
- [39] O. V. Skryabina, S. V. Egorov, A. S. Goncharova, A. A. Klimenko, S. N. Kozlov, V. V. Ryazanov, S. V. Bakurskiy, M. Y. Kupriyanov, A. A. Golubov, K. S. Napolskii, and V. S. Stolyarov, Josephson coupling across a long single-crystalline Cu nanowire, *Applied Physics Letters* **110**, 222605 (2017).
- [40] Y. S. Barash, Phase relations in superconductor–normal metal–superconductor tunnel junctions, *Phys. Rev. B* **99**, 140508 (2019).
- [41] I. Soloviev, S. Bakurskiy, V. Ruzhickiy, N. Klenov, M. Kupriyanov, A. Golubov, O. Skryabina, and V. Stolyarov, Miniaturization of Josephson junctions for digital superconducting circuits, *Phys. Rev. Applied* **16**, 044060 (2021).
- [42] A. F. Volkov, Weak coupling produced in superconductors by irradiation, *Zh. Eksp. Teor. Fiz.* **60**, 1500 (1971), [*Sov. Phys. JETP* **33**, 811 (1971)].
- [43] H. J. Fink, Supercurrents through superconducting-normal-superconducting proximity layers. I. Analytic solution, *Phys. Rev. B* **14**, 1028 (1976).
- [44] M. Y. Kupriyanov and V. F. Lukichev, Influence of boundary transparency on the critical current of “dirty” SS'S structures, *Sov. Phys. JETP* **67**, 1163 (1988).
- [45] I. Petković, A. Lollo, L. I. Glazman, and J. Harris, Deterministic phase slips in mesoscopic superconducting rings, *Nature Communications* **7**, 13551 (2016).
- [46] L. G. Aslamazov and A. I. Larkin, Josephson effect in superconducting point contacts, *JETP Lett.* **9**, 87 (1969).
- [47] P. G. de Gennes, *Superconductivity of Metals and Alloys* (Addison Wesley, Reading, MA, 1966).
- [48] S.-K. Yip, O. F. De Alcantara Bonfim, and P. Kumar, Supercurrent tunneling between conventional and unconventional superconductors: A Ginzburg-Landau approach, *Phys. Rev. B* **41**, 11214 (1990).
- [49] M. Sigrist and K. Ueda, Phenomenological theory of unconventional superconductivity, *Rev. Mod. Phys.* **63**, 239 (1991).
- [50] E. M. Lifshitz and L. P. Pitaevskii, *Statistical Physics. Part 2. Theory of the Condensed State* (Butterworth-Heinemann, Oxford, 1995).
- [51] V. P. Mineev and K. Samokhin, *Introduction to Unconventional Superconductivity* (Gordon & Breach Science Publishers, New York, 1999).
- [52] M. Tinkham, *Introduction to Superconductivity*, 2nd ed. (McGraw-Hill, New York, 1996).
- [53] A. Barone and G. Paterno, *Physics and Applications of the Josephson Effect* (John Wiley&Sons, New York, 1982).
- [54] R. O. Zaitsev, Boundary conditions for the superconductivity equations at temperatures close to critical, *Sov. Phys. JETP* **21**, 1178 (1965).
- [55] Z. G. Ivanov, M. Y. Kupriyanov, K. K. Likharev, S. V. Meriakri, and O. V. Snigirev, Boundary conditions for the Usadel and Eilenberger equations, and properties of dirty SNS sandwich-type junctions, *Sov. J. Low Temp. Phys.* **7**, 274 (1981).
- [56] T. Tokuyasu, J. A. Sauls, and D. Rainer, Proximity effect of a ferromagnetic insulator in contact with a superconductor, *Phys. Rev. B* **38**, 8823 (1988).
- [57] A. Cottet, D. Huertas-Hernando, W. Belzig, and Y. V. Nazarov, Spin-dependent boundary conditions for isotropic superconducting Green's functions, *Phys. Rev. B* **80**, 184511 (2009).
- [58] A. Samoilenka and E. Babaev, Boundary states with elevated critical temperatures in Bardeen-Cooper-Schrieffer superconductors, *Phys. Rev. B* **101**, 134512 (2020).
- [59] M. D. Croitoru, A. A. Shanenko, Y. Chen, A. Vagov, and J. A. Aguiar, Microscopic description of surface superconductivity, *Phys. Rev. B* **102**, 054513 (2020).
- [60] A. Samoilenka and E. Babaev, Microscopic derivation of superconductor-insulator boundary conditions for Ginzburg-Landau theory revisited: Enhanced superconductivity at boundaries with and without magnetic field, *Phys. Rev. B* **103**, 224516 (2021).
- [61] L. J. Buchholtz and G. Zwicknagl, Identification of p -wave superconductors, *Phys. Rev. B* **23**, 5788 (1981).
- [62] Y. S. Barash, A. V. Galaktionov, and A. D. Zaikin, Charge transport in junctions between d -wave superconductors, *Phys. Rev. B* **52**, 665 (1995).
- [63] M. Matsumoto and H. Shiba, On boundary effect in d -wave superconductors, *J. Phys. Soc. Jpn.* **64**, 1703 (1995).
- [64] M. Matsumoto and H. Shiba, Coexistence of different symmetry order parameters near a surface in d -wave superconductors I, *J. Phys. Soc. Jpn.* **64**, 3384 (1995).
- [65] M. Matsumoto and H. Shiba, Coexistence of different symmetry order parameters near a surface in d -wave superconductors II, *J. Phys. Soc. Jpn.* **64**, 4867 (1995).
- [66] M. Matsumoto and H. Shiba, Coexistence of different symmetry order parameters near a surface in d -wave superconductors III, *J. Phys. Soc. Jpn.* **65**, 2194 (1996).
- [67] Y. Nagato and K. Nagai, Surface and size effect of a d_{xy} -state superconductor, *Phys. Rev. B* **51**, 16254 (1995).
- [68] L. J. Buchholtz, M. Palumbo, D. Rainer, and J. A. Sauls, Thermodynamics of a d -wave superconductor near a surface, *J. Low Temp. Phys.* **101**, 1079 (1995).
- [69] L. J. Buchholtz, M. Palumbo, D. Rainer, and J. A. Sauls, The effect of surfaces on the tunneling density of states of an anisotropically paired superconductor, *J. Low Temp. Phys.* **101**, 1099 (1995).
- [70] M. Alber, B. Bäuml, R. Ernst, D. Kienle, A. Kopf, and M. Rouchal, Surface boundary conditions for the Ginzburg-Landau theory of d -wave superconductors, *Phys. Rev. B* **53**, 5863 (1996).
- [71] D. F. Agterberg, Extrapolation lengths of unconventional superconductors, *Journal of Physics: Condensed Matter* **9**, 7435 (1997).
- [72] Y. S. Barash, Anharmonic Josephson current in junctions with an interface pair breaking, *Phys. Rev. B* **85**, 100503 (2012).

- [73] Y. S. Barash, Probing interfacial pair breaking in tunnel junctions based on the first and the second harmonics of the Josephson current, *Phys. Rev. B* **85**, 174529 (2012).
- [74] Y. S. Barash, Non-Fraunhofer patterns of the anharmonic Josephson current influenced by strong interfacial pair breaking, *Phys. Rev. B* **86**, 144502 (2012).
- [75] Y. S. Barash, Magnetic penetration depth and vortex structure in anharmonic superconducting junctions with an interfacial pair breaking, *Phys. Rev. B* **89**, 174516 (2014).
- [76] Y. S. Barash, Interfacial pair breaking and planar weak links with an anharmonic current-phase relation, *JETP Lett.* **100**, 205 (2014).
- [77] Y. S. Barash, Proximity-induced minimum radius of superconducting thin rings closed by the Josephson 0 or π junction, *Phys. Rev. B* **95**, 024503 (2017).
- [78] L. P. Gor'kov, Microscopic derivation of the Ginzburg-Landau equations in the theory of superconductivity, *JETP* **9**, 1364 (1959).
- [79] L. P. Gor'kov, Theory of superconducting alloys in a strong magnetic field near the critical temperature, *JETP* **10**, 998 (1960).
- [80] A. A. Abrikosov, *Fundamentals of the Theory of Metals* (North Holland, Amsterdam, 1988).
- [81] A. Buzdin, Direct coupling between magnetism and superconducting current in the Josephson φ_0 junction, *Phys. Rev. Lett.* **101**, 107005 (2008).
- [82] A. Zazunov, R. Egger, T. Jonckheere, and T. Martin, Anomalous Josephson current through a spin-orbit coupled quantum dot, *Phys. Rev. Lett.* **103**, 147004 (2009).
- [83] J.-F. Liu and K. S. Chan, Relation between symmetry breaking and the anomalous Josephson effect, *Phys. Rev. B* **82**, 125305 (2010).
- [84] D. B. Szombati, S. Nadj-Perge, D. Car, S. R. Plissard, E. P. A. M. Bakkers, and L. P. Kouwenhoven, Josephson φ_0 -junction in nanowire quantum dots, *Nature Physics* **12**, 568 (2016).
- [85] M. A. Silaev, I. V. Tokatly, and F. S. Bergeret, Anomalous current in diffusive ferromagnetic Josephson junctions, *Phys. Rev. B* **95**, 184508 (2017).
- [86] S. Mironov and A. Buzdin, Spontaneous currents in superconducting systems with strong spin-orbit coupling, *Phys. Rev. Lett.* **118**, 077001 (2017).
- [87] V. M. Edelstein, The Ginzburg - Landau equation for superconductors of polar symmetry, *Journal of Physics: Condensed Matter* **8**, 339 (1996).
- [88] K. V. Samokhin, Magnetic properties of superconductors with strong spin-orbit coupling, *Phys. Rev. B* **70**, 104521 (2004).
- [89] R. P. Kaur, D. F. Agterberg, and M. Sigrist, Helical vortex phase in the noncentrosymmetric CePt_3Si , *Phys. Rev. Lett.* **94**, 137002 (2005).
- [90] V. M. Edelstein, Ginzburg-Landau theory for impure superconductors of polar symmetry, *Phys. Rev. B* **103**, 094507 (2021).
- [91] V. Ambegaokar and A. Baratoff, Tunneling between superconductors, *Phys. Rev. Lett.* **10**, 486 (1963); Tunneling between superconductors, **11**, 104 (1963).
- [92] V. P. Galaiko, A. V. Svidzinskii, and V. A. Slyusarev, Concerning the theory of proximity effects in superconductors, *Sov. Phys. JETP* **29**, 454 (1969).
- [93] E. N. Bratus' and A. V. Svidzinskii, Josephson current in superconductors with nonmagnetic impurities, *Teor. Math. Phys.* **30**, 153 (1977).
- [94] A. V. Svidzinskii, *Spatially Non-Uniform Problems in the Theory of Superconductivity* (Nauka, Moscow, 1982) [in Russian].
- [95] E. V. Bezuglyi, E. N. Bratus', and V. P. Galaiko, On the theory of Josephson effect in a diffusive tunnel junction, *Low Temp. Phys.* **25**, 167 (1999).
- [96] E. V. Bezuglyi, A. S. Vasenko, V. S. Shumeiko, and G. Wendin, Nonequilibrium effects in tunnel Josephson junctions, *Phys. Rev. B* **72**, 014501 (2005).
- [97] M. Y. Kupriyanov, Effect of a finite transmission of the insulating layer on the properties of SIS tunnel junctions, *JETP Lett.* **56**, 399 (1992).
- [98] V. B. Geshkenbein, Vortex interaction with a twinning boundary in a superconductor, *Sov. Phys. JETP* **67**, 2166 (1988).
- [99] A. A. Abrikosov, On the magnetic properties of superconductors of the second group, *Sov. Phys. JETP* **5**, 1174 (1957).
- [100] P. de Gennes, Self-consistent calculation of the Josephson current, *Physics Letters* **5**, 22 (1963).
- [101] G. Deutscher and P. G. de Gennes, in *Superconductivity*, Vol. 2, edited by R. D. Parks (Marcel Dekker, Inc., New York, 1969) p. 1005.
- [102] V. L. Ginzburg and L. P. Pitaevskii, On the theory of superfluidity, *Soviet Physics JETP* **34**, 858 (1958).
- [103] E. A. Andryushin, V. L. Ginzburg, and A. P. Silin, Boundary conditions in the macroscopic theory of superconductivity, *Usp. Fiz. Nauk* **163**, 105 (1993), [*Phys-Usp* **36**, 854-857 (1993)].
- [104] R. De Luca and F. Romeo, Sawtooth current-phase relation of a superconducting trilayer system described using Ohta's formalism, *Phys. Rev. B* **79**, 094516 (2009).
- [105] A. Y. Kitaev, Unpaired majorana fermions in quantum wires, *Physics-Uspekhi* **44**, 131 (2001).
- [106] L. Fu and C. L. Kane, Josephson current and noise at a superconductor/quantum-spin-Hall-insulator/superconductor junction, *Phys. Rev. B* **79**, 161408 (2009).
- [107] C. Beenakker, Search for Majorana fermions in superconductors, *Annual Review of Condensed Matter Physics* **4**, 113 (2013).
- [108] J. Alicea, New directions in the pursuit of Majorana fermions in solid state systems, *Reports on Progress in Physics* **75**, 076501 (2012).

- [109] J. Wiedenmann, E. Bocquillon, R. S. Deacon, S. Hartinger, O. Herrmann, T. M. Klapwijk, L. Maier, C. Ames, C. Brüne, C. Gould, A. Oiwa, K. Ishibashi, S. Tarucha, H. Buhmann, and L. W. Molenkamp, 4π -periodic Josephson supercurrent in HgTe-based topological Josephson junctions, *Nature Communications* **7**, 10303 (2016).
- [110] E. Bocquillon, R. S. Deacon, J. Wiedenmann, P. Leubner, T. M. Klapwijk, C. Brüne, K. Ishibashi, H. Buhmann, and L. W. Molenkamp, Gapless Andreev bound states in the quantum spin Hall insulator HgTe, *Nature Nanotechnology* **12**, 137 (2017).
- [111] J. A. Blackburn, B. B. Schwartz, and A. Baratoff, Single and multiple superconducting weak-link systems, *Journal of Low Temperature Physics* **20**, 523 (1975).
- [112] Y. S. Way, K. S. Hsu, and Y. H. Kao, Interactions between two superconducting weak links in the stationary ($v = 0$) states, *Phys. Rev. Lett.* **39**, 1684 (1977).
- [113] I. Zapata and F. Sols, Supercurrent flow through an effective double-barrier structure, *Phys. Rev. B* **53**, 6693 (1996).